Journal of Biomedical Materials Research Part A

WILEY

Society For Biomaterials

RESEARCH ARTICLE OPEN ACCESS

Comparative Analysis of Hydrogels From Porcine Extracellular Matrix for 3D Bioprinting of Adipose Tissue

Leonie Füge[1] | Felix Schüssler[1] | Jamina Gerhardus[2] | Roxana Schwab[1] | Gregory Harms[3,4] | Annette Hasenburg[1] | Andreas Blaeser[2,5] | Walburgis Brenner[1,6] | Katharina Peters[1,6]

[1]Department of Obstetrics and Women's Health, University Medical Center of the Johannes Gutenberg University Mainz, Mainz, Germany | [2]BioMedical Printing Technology, Department of Mechanical Engineering, Technical University of Darmstadt, Darmstadt, Germany | [3]Cell Biology Unit, University Medical Center of the Johannes Gutenberg University Mainz, Mainz, Germany | [4]Department of Biology, Wilkes University, Wilkes Barre, Pennsylvania, USA | [5]Centre for Synthetic Biology, Technical University of Darmstadt, Darmstadt, Germany | [6]BiomaTiCS – Biomaterials, Tissues and Cells in Science, University Medical Center of the Johannes Gutenberg University Mainz, Mainz, Germany

Correspondence: Katharina Peters (katharina.peters@unimedizin-mainz.de)

Received: 31 July 2024 | **Revised:** 19 October 2024 | **Accepted:** 24 October 2024

Funding: The authors received no specific funding for this work.

Keywords: 3D bioprinting | adipose tissue | decellularization | extracellular matrix | hydrogel | tissue engineering | vascularization

ABSTRACT

The extracellular matrix (ECM) is the natural scaffold of all soft tissues in tissue engineering. Of special interest is the use of ECM as a hydrogel, which can be used to enclose cells and to be molded into any form by 3D bioprinting. Protocols for the preparation of ECM vary in the use of physical and chemical processing steps, the use of different detergents for decellularization, and the removal of DNA and RNA residues and show a different use of solvents and wash buffers. We have, therefore, compared seven different variations for the decellularization of a primary porcine isolate to manufacture decellularized adipose tissue (DAT) for their use in adipose tissue engineering and as a hydrogel in particular. Decellularization efficacy was assessed by DNA quantification while retention of ECM components was evaluated by measuring the content of hydroxyproline and glycosaminoglycan (GAGs). Depending on the decellularization protocol, the composition and DNA content of the resulting DAT were different. All DAT samples were processed into hydrogels to assess their mechanical properties as well as their influence on cellular metabolic activity and cell differentiation. The different compositions of the DAT and the resulting hydrogels had an effect on the stability and printability of the gels. Some DAT that were digested with hydrochloric acid (HCl) were more stable than those that were digested with acetic acid (AA). In addition, depending on the protocol, there was a clear effect on adipose-derived stem cells (ASC), endothelial cells and fibroblasts, cultured with the hydrogels. The differentiation of ASC to adipocytes could be achieved on most of the hydrogels. Human dermal microvascular endothelial cells (HDMEC) showed significantly better metabolic activity on hydrogels digested with HCl than digested with AA. HDMEC cultured on hydrogel #2 digested with HCl showed a 40% higher metabolic activity compared to collagen as a positive control, whereas culturing HDMEC on hydrogel #2 digested with AA resulted in a cellular metabolic activity loss of 60%. In a triculture of all three cell types, the formation of first tubular networks by HDMEC was achieved depending on the hydrogel used.

1 | Introduction

The reconstruction of soft tissue defects caused by tumors, trauma, or malformations, continues to make up a major hurdle in regenerative medicine [1, 2]. Particularly in breast reconstruction, standard care practices consisting of autologous adipose tissue transfers or implants are associated with a variety of disadvantages. Donor site morbidity, flap failure, capsular

contracture, and implant rupture may occur leading to reoperation rates as high as 70% within the first 10 years [3]. Even though it is effective for small volumes and the correction of contour defects, autologous fat grafting is limited by poor volume retention [4]. This is due to necrosis, calcifications, and oil cyst formation of the highly oxygen-dependent adipose tissue without adequate vascularization [5].

Tissue engineering of adipose tissue has emerged as a promising alternative to address these disadvantages [1, 6]. Typically, a suitable scaffold material is seeded with autologous cells to support the body in its regeneration of the tissue while avoiding foreign body reactions [1, 7, 8]. Multipotent adipose-derived stem cells are used as the primary cellular component, due to their high abundance, simple extraction with low donor site morbidity, and their adipogenic, angiogenetic, and highly regenerative properties [9–14].

The extracellular matrix (ECM) is the natural scaffold of all tissues. Its complex composition serves as structural support while mediating site-specific cellular growth, differentiation, and function in the dynamic coexistence of the cells [15–17]. It is mainly comprised of collagen, fibronectin, laminin, elastin, and glycosaminoglycans (GAGs) and in addition contains various growth factors and cytokines [16, 18]. To date, no universally applicable scaffold material has been described, that can fully recapitulate the complex composition and function of the ECM [19].

This has led to approaches where the native ECM itself is reused as a scaffold material that inherently possesses the required features [16, 17, 20]. Extracellular matrix scaffolds have been successfully employed for almost every tissue of the body [21]. They can be used in a variety of forms such as sheets, powders, foams, and microcarriers [16, 17, 22]. Of special interest is the use of ECM as a hydrogel, which can be used to enclose cells and to be molded into any form by 3D bioprinting [23, 24]. To avoid unwanted immunogenicity and inflammatory response, the ECM must be freed of resident cells and immunogenic components, such as remaining nucleic acids and cellular debris [25, 26]. This decellularization typically uses a combination of physical, chemical, and enzymatic treatments [20, 27]. These aggressive treatments can damage the ECM. This is why the process needs to be carefully balanced to ensure adequate decellularization while preserving the ECM as much as possible. There is no universally applicable method since every tissue is unique in its composition and requires individually adapted protocols [20, 21, 27, 28].

Since the first description by Flynn [29], various groups have developed protocols to obtain decellularized extracellular matrix from adipose tissue for soft tissue engineering (Reviewed by [30]). Favorable outcomes regarding viability and proliferation [31–33], adipogenesis [29, 31, 33–37], angiogenesis [35, 38, 39] and wound healing [40, 41] have been reported using decellularized adipose tissue (DAT), particularly in combination with human adipose-derived mesenchymal stem cells (ASC). However, decellularization protocols vary widely with no consensus regarding the most appropriate method, and only limited comparisons have been reported [42–44].

We, therefore, set out to compare different variations for the decellularization of the primary isolate to manufacture decellularized adipose tissue (DAT). We were guided by the protocols described in the literature for use in adipose tissue engineering and, in particular, as a hydrogel for future 3D bioprinting. Porcine adipose tissue was chosen as donor material since it can be easily obtained from the meat industry to allow for an off-the-shelf product. Autologous or discarded human adipose tissue is also often considered, but donor differences such as age and obesity status may lead to higher variability than a xenogenic product from a controlled environment [45]. Even though xenoantigens such as the α-1,3-galactose disaccharide (α-Gal) epitope could potentially induce undesirable immune responses, this can be avoided by complete decellularization as can be seen by the wide clinical application of decellularized xenografts [46–49]. In our work, decellularization efficacy was assessed by DNA quantification, and retention of ECM components was evaluated by measuring the protein or rather the content of hydroxyproline and glycosaminoglycans (GAGs). All DAT materials were processed into hydrogels to assess their mechanical properties and cellular reactions. In addition to the behavior of ASC, compatibility with human dermal microvascular endothelial cells (HDMEC) was investigated. The compatibility and use of endothelial cells in tissue engineering are necessary to vascularize the hydrogels, which are provided with adipocytes in vitro [50]. The long-term goal is a triculture of autologous ASC, endothelial cells and fibroblasts, which additionally support the formation of the ECM [51], in a suitable printable hydrogel for adipose tissue reconstruction.

2 | Materials & Methods

2.1 | Extraction of Extracellular Matrix From Porcine Adipose Tissue

Protocols in literature use different tissues with varying properties and thus differ in their pre-processing before the actual decellularization. We therefore developed a pre-processing protocol to obtain a "primary isolate", that was adequate even for protocols developed for much softer tissue samples or lipoaspirate. Porcine dorsal fat was obtained from a local slaughterhouse (Hofgut Acker, Bodenheim, Germany) on the day of slaughter and immediately processed. The fat was cooled down for about 20 min at −20°C to firm up and ease processing. After removing the dermis and any remaining muscular tissue, the fat was cut into 2 × 2 × 2 cm pieces, and the surface was decontaminated by a 70% ethanol wash, followed by two doubly distilled (dd)H_2O washes. Afterward, the tissue was finely minced using a commercial meat grinder. 500 g of minced fat was homogenized in 1 L of 37°C ddH_2O, and the resulting slurry was strained through a 1 mm sieve. The resulting white fibrous tissue was washed in 37°C tap water until the fatty parts were removed. The tissue was decontaminated again for 10 min in 70% ethanol, centrifuged at 1000 g for 5 min, and washed 3 times in ddH_2O or until no more lipids were visible after centrifugation (1500 g, 5 min). After the last washing step, the resulting fibrous tissue (primary isolate) was centrifuged for 10 min at 4000 g to remove excess moisture, weighted, distributed equally across decellularization protocols, and frozen at −80°C until use (Figure 1).

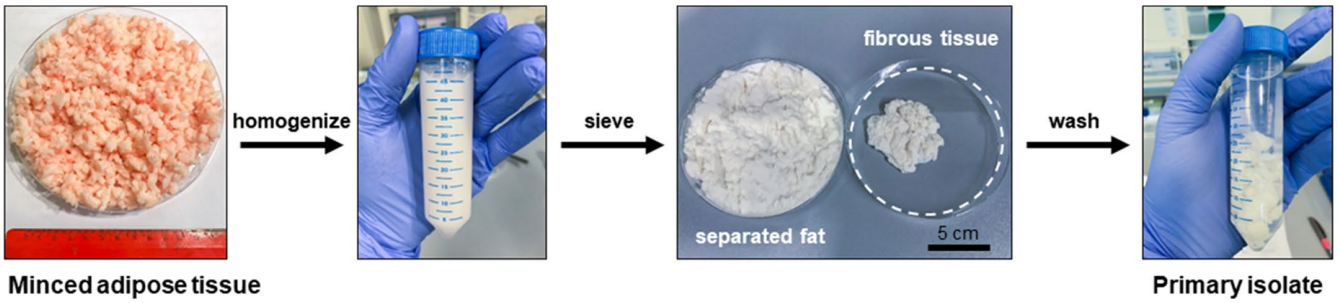

FIGURE 1 | Schematic illustration of the processing steps to obtain primary isolate from native adipose tissue.

2.2 | Decellularization of Extracellular Matrix

Different methods for decellularization of the obtained primary isolate were performed to be compared with each other (Table 1). Various protocols from seven different publications [29, 31, 35, 36, 42, 52, 53] were used as a basis with modifications for this purpose. All isolation steps were carried out in 50 mL conical tubes on a shaker at 37°C to soften the tissue. 5 g of primary isolate was used per tube and solutions filled up to the 50 mL mark. To change liquids, samples were centrifuged (1500 g for 5 min). If the solid tissue could not be separated by centrifugation, the liquid was removed using a 100 μm cell strainer (Greiner Bio-One). After the decellularization protocols, samples were frozen at −80°C until freeze-drying (Alpha 2–4 LDplus, Christ). Freeze-dried samples were snap-frozen in liquid nitrogen and milled using an electric spice grinder, taking care not to overheat samples. Static charges from lyophilization could be countered by using an anti-static gun (Zerostat 3, Milty). The pulverized samples were weighted to calculate yield in reference to the primary isolate (wet weight) and stored at −80°C until further use. In the following, all steps were carried out at room temperature unless otherwise specified.

2.2.1 | Decellularization Protocol #1

The method for preparing decellularized adipose tissue (DAT) #1 is based on the isolation protocol of Brown et al. "Method A" [42]. The described pre-processing of freezing at −80°C and cutting into thin slices using a rotary blade described by Brown et al. was replaced by the primary isolate isolation described above in order to standardize the starting procedure. After thawing, the tissue was washed in water before treatment with 0.25% trypsin/EDTA (T4049, Sigma-Aldrich), 3% Triton-X 100 (9002-93-1, Sigma-Aldrich) and 4% sodium deoxycholate (3484.1, Carl Roth) solutions for 1 h each and water washes in between. After storage in water at 4°C overnight, the tissue was disinfected for 2 h in a 4% ethanol 0.1% peracetic acid (257,750,250, Thermo Fisher Scientific) solution. After DPBS and water washes, the intermediate lyophilization step was omitted and the lipids were removed for 1 h in n-propanol. After thorough washing with water, the tissue was frozen at −80°C before lyophilization.

2.2.2 | Decellularization Protocol #2

Processing of DAT #2 is based on the protocol of Edri et al. [52]. The publication describes a method to generate hydrogel from porcine and human omentum tissues and was included due to the fatty composition of the tissue. Samples were lysed in hypotonic Tris-EDTA buffer (10 mM Tris, 5 mM EDTA, pH 8) supplemented with 1 mM phenylmethylsulfonyl fluoride (PMSF, P7626-16, Sigma-Aldrich) followed by three freeze–thaw cycles (−80°C to room temperature) in the same buffer, with buffer changes after each cycle. Afterward, the tissue was washed in 70% ethanol and 100% ethanol for 30 min each, before lipid extraction by 3 × 30 min acetone washes, followed by 24 h in a 60/40 (v/v) mixture of hexane (3907.1, Roth) and acetone (131007.1212, AppliChem) with one change. The tissue was washed again in 100% ethanol for 30 min followed by 70% ethanol at 4°C overnight. After 4 × DPBS washes, the tissue was incubated overnight with 0.25% trypsin/EDTA solution. The tissue was washed again in DPBS before 24 h hyperosmolar treatment with 1.5 M NaCl solution with three changes. After a DPBS washing step, the tissue was treated with a 5 mM Tris/1% Triton-X 100 (pH 8) solution for 1 h before extensive washing in DPBS and ddH_2O. The tissue was disinfected in 70% ethanol, thoroughly washed in water, and frozen at −80°C before lyophilization.

2.2.3 | Decellularization Protocol #3

Processing of DAT #3 is based on the protocol of Wang et al. [53]. They described the decellularization of excised human adipose tissue blocks. In their application, the decellularized matrices were not turned into a hydrogel but rather lyophilized, crushed and the microparticles mixed with saline for injection. The tissue was subjected to 3 × freeze–thaw cycles (−80°C to room temperature), followed by a 48 h wash in ddH_2O with changes every 12 h. 1% penicillin/streptomycin solution (P0781, Sigma-Aldrich) was added to prevent microbial growth at 37°C. Samples were treated with 0.5 M NaCl solution for 4 h and then again with 1 M NaCl solution for 4 h, followed by an overnight water wash twice in a row. After incubation with 0.25% trypsin/EDTA solution for 1 and a 1 h water wash, lipids were removed by isopropanol treatment overnight. The tissue was then treated with 1% Triton-X 100 for 3 days with daily change, followed by a 48 h water wash, again supplemented by 1% penicillin/streptomycin. Again, the tissue was disinfected in 70% ethanol, thoroughly washed in water, and frozen at −80°C before lyophilization.

2.2.4 | Decellularization Protocol #4

Processing of DAT #4 is based on the protocol of Pati et al. [35]. The publication describes the use of human lipoaspirate for

TABLE 1 | Steps of the different decellularization protocols #1–#7. Listed are the decellularization processes we performed based on the methods we modified from Brown et al. (protocol #1), Edri et al. (protocol #2), Wang et al. (protocol #3), Pati et al. (protocol #4), Tan et al. (protocol #5), Choi et al. (protocol #6), and Flynn et al. (protocol #7).

Step	Protocol #1	Protocol #2	Protocol #3	Protocol #4	Protocol #5	Protocol #6	Protocol #7
1	0.25% Trypsin/EDTA, 1 h	DPBS wash	Freeze–thaw, 3 x	DPBS wash, 3×5 min	Cryo-mill	1.5 M NaCl, 24 h, 1 change	Freeze–thaw, 3×, 10 mM Tris, 5 mM EDTA, 1% Antibiotic/Antimycotic (ABAM), 14 μM PMSF, pH 8
2	ddH_2O, 1×5 min, 1×15 min, 1×30 min	10 mM Tris, 5 mM EDTA, 1 mM PMSF, pH 8, 1 h	ddH_2O, *1% penicillin–streptomycin*, 48 h, change every 12 h	0.5% SDS, 48 h, change every 12 h	DPBS wash, 3×5 min	ddH_2O, 1×5 min, 1×15 min, 1×30 min	DPBS, 14 μM PMSF, 3×5 min
3	3% Triton X-100, 1 h	Freeze–thaw, 3×, 10 mM Tris, 5 mM EDTA, 1 mM PMSF, pH 8	0.5 M NaCl, 4 h	DPBS wash, 3×5 min	0.5% SDS, 4 h, 1 change	0.5% SDS, 24 h, change 1×	0.25% Trypsin/EDTA, 1% ABAM, 16 h
4	ddH_2O, 1×5 min, 1×15 min, 1×30 min	70% ethanol, 30 min	1 M NaCl, 4 h	Isopropanol, 48 h, change every 12 h	DPBS wash, 3×5 min	ddH_2O, 1×5 min, 1×15 min, 1×30 min	DPBS, 14 μM PMSF, 1×5 min, 1×15 min, 1×30 min
5	4% deoxycholic acid, 1 h	100% ethanol, 30 min	ddH_2O, overnight	DPBS wash, 3×15 min	Isopropanol, 2h, 1 change	66.67 U/mL DNase I 62.5 μg/mL RNase A, 24 h	Isopropanol, 1% ABAM, 14 μM PMSF, 48 h, change every 12 h
6	ddH_2O, 1×5 min, 1×15 min, 1×30 min	100% acetone, 3×30 min	0.5 M NaCl, 4 h	4% ethanol, 0.1% peracetic acid, 4 h	DPBS wash, 1×5 min, 1×15 min, 1×30 min	ddH_2O, 1×5 min, 1×15 min, 1×30 min	SPB rinse 1% ABAM, 14 μM PMSF, 3×30 min
7	Store in ddH_2O, 4°C, overnight	60% hexane, 40% acetone, 24 h, 1 change	1 M NaCl, 4 h	DPBS wash, 3×15 min	70% ethanol, 1×5 min, 1×15 min, 1×30 min	70% ethanol, 1×5 min, 1×15 min, 1×30 min	0.25% Trypsin/EDTA, 6 h
8	4% ethanol, 0.1% peracetic acid, 2 h	100% ethanol, 30 min	ddH_2O, overnight	ddH_2O, 1×5 min, 1×15 min, 1×30 min, 1× overnight, 1×2 h	ddH_2O, 1×5 min, 1×15 min, 1×30 min, 1× overnight, 1×2 h	ddH_2O, 1×5 min, 1×15 min, 1×30 min, 1× overnight, 1×2 h	SPB rinse, 1% ABAM, 14 μM PMSF, 3×30 min
9	DPBS, 3×15 min	70% ethanol, overnight, 4°C	0.25% Trypsin/EDTA, 1 h	Lyophilize	Lyophilize	Lyophilize	66.67 U/mL DNase I, 62.5 μg/mL RNase A, 20 U/mL lipase type VI-S, 55 mM Na_2HPO_4, 17 mM KH_2PO_4, 4.9 mM $MgSO_4$ 1% ABAM, 14 μM PMSF, 16 h

(Continues)

TABLE 1 | (Continued)

Step	Protocol #1	Protocol #2	Protocol #3	Protocol #4	Protocol #5	Protocol #6	Protocol #7
10	ddH_2O, 2×15 min	DPBS wash, 4×	ddH_2O, 1 h				SPB rinse, 1% ABAM, 14 μM PMSF, 3×30 min
11	N-propanol, 1 h	0.25% Trypsin/EDTA, overnight	Isopropanol, overnight, *1 change*				Isopropanol, 1% ABAM, 14 μM PMSF, 8 h
12	ddH_2O, 1×5 min, 1×15 min, 1×30 min, 1×overnight, 1×2 h	DPBS, 1×5 min, 1×15 min, 1×30 min	ddH_2O, 3×5 min				SPB rinse, 1% ABAM, 14 μM PMSF, 3×30 min
13	Lyophilize	1.5 M NaCl, 24 h, three changes	1% Triton-X 100, 3 days, change daily				70% ethanol, 3×30 min
14		DPBS wash, 1×15 min	ddH_2O, 1% *penicillin–streptomycin*, 48 h, 3 change per day				ddH_2O, 1×5 min, 1×15 min, 1×30 min, 1×overnight, 1×2 h
15		5 mM Tris, 1% Triton-X 100, pH 8, 1 h	70% ethanol, 1×5 min, 1×15 min, 1×30 min				Lyophilize
16		DPBS wash, 1×5 min, 1×15 min, 1×30 min	ddH_2O, 1×5 min, 1×15 min, 1×30 min, 1×overnight, 1×2 h				
17		ddH_2O, 1×5 min, 1×15 min, 1×30 min	Lyophilize				
18		70% ethanol, 1×5 min, 1×15 min, 1×30 min					
19		ddH_2O, 1×5 min, 1×15 min, 1×30 min, 1×overnight, 1×2 h					
20		Lyophilize					

the generation of a hydrogel. After 3 × DPBS washes, the tissue was subjected to 48 h decellularization by 0.5% sodium dodecyl sulfate (SDS, A3942, AppliChem) with solution changes every 12 h. A brief DPBS washing step was introduced to the original protocol to ensure that a large part of the SDS had already been removed before lipid extraction by 48 h isopropanol, with changes every 12 h, was carried out. After further DPBS washes, the tissue was sterilized for 4 h in a 4% ethanol and 0.1% peracetic acid solution. After thorough DPBS and ddH_2O washes, the tissue was frozen at −80°C before lyophilization.

2.2.5 | Decellularization Protocol #5

Processing of DAT #5 is based on the protocol of Tan et al. [36]. They describe the generation of a hydrogel from porcine adipose tissue. During pre-processing, homogenization and collection of tissue by centrifugation was performed. Additionally, the tissue was cryo-milled before the extraction to increase surface area and speed up the process. Since the decellularization agents are very similar to the Pati protocol, this mechanical pre-processing was included to compare the impact on decellularization. The primary isolate was frozen in liquid nitrogen and cryo-milled by impact crushing (Cellcrusher). The pulverized samples were washed in DPBS and subjected to 4 h of 0.5% SDS treatment, whereby the SDS solution was exchanged once. After a brief wash in DPBS, the lipids were removed by soaking for 2 h in isopropanol with one change of solution. The tissue was washed again in DPBS, disinfected in 70% ethanol, thoroughly washed in water, and frozen at −80°C before lyophilization.

2.2.6 | Decellularization Protocol #6

Processing of DAT #6 is based on the protocol of Choi et al. [31]. They describe a method to decellularize porcine adipose tissue to generate a porous scaffold without a solvent-based lipid removal step. Similar to the mechanical pre-processing described here, the tissue is chopped and homogenized, and a majority of fat is removed by centrifugation before decellularization. The tissue was then subjected to 1.5 M NaCl solution for 24 h with one change of solution. A ddH_2O wash step was introduced to reduce salt levels, and the tissue was treated with 0.5% SDS for 24 h, with one change of solution. After additional ddH_2O washes, DNA and RNA remains were removed by combined DNase (DNase I, 66.67 U/mL, D4527, Sigma-Aldrich) and RNase (RNase A, 62.5 μg/mL, R5125, Sigma-Aldrich) treatment. Since enzymes and a buffer were not clearly specified by Choi et al. [31] concentrations, and buffers were adapted from Flynn et al. [29, 54]. After three washes in ddH_2O, the tissue was disinfected in 70% ethanol, again thoroughly washed in ddH_2O, and frozen at −80°C before lyophilization.

2.2.7 | Decellularization Protocol #7

Processing of DAT #7 is based on the protocol of Flynn et al. [29]. A detailed description of the detergent-free method can be found in Morisette Martin et al. [54] and includes further processing into hydrogels, microbeads, and foams from DAT. In the original publication, the excised tissue was cut into 20–25 g pieces, which was replaced by primary isolate isolation, as described above. The tissue was subjected to 3 × freeze–thaw cycles in 10 mM Tris/5 mM EDTA buffer (pH 8) and supplemented with 14 μM of the protease inhibitor phenylmethylsulfonyl fluoride (PMSF) and antibiotic/antimycotic solution (ABAM, A5955, Sigma-Aldrich) with solution changes after each cycle. A brief DPBS/PMSF wash was introduced before digesting the tissue with 0.25% trypsin/EDTA with 1% ABAM for 16 h. After another DPBS/PMSF wash, lipids were removed by isopropanol (supplemented with ABAM and PMSF) treatment for 48 h, changing the solution twice a day. The isopropanol was removed by three Sorensen's phosphate buffers (SPB: 8 g/L NaCl, 200 mg/L KCl, 1 g/L Na2HPO4, 200 mg/L KH_2PO_4, 1% ABAM, 14 μM PMSF) washes and digested again for 6 h in trypsin/EDTA. The tissue was rinsed in SPB before enzymatic removal of DNA, RNA, and lipids by incubation with 66.67 U/mL DNase I, 62.5 μg/mL RNase A, 20 U/mL lipase type VI-S (L0382, Sigma-Aldrich) in 55 mM Na_2HPO_4, 17 mM KH_2PO_4, 4.9 mM $MgSO_4$, 1% ABAM and 14 μM PMSF for 16 h. After additional washes in SPB, the tissue was treated with isopropanol for another 8 h and rinsed again. The tissue was then disinfected in 70% ethanol, thoroughly washed in ddH_2O, and frozen at −80°C before lyophilization.

2.3 | Papain Digestion

DAT samples were papain digested to analyze total DNA, hydroxyproline and glycosaminoglycan content. 25 mg/mL per sample were digested with 250 μg/mL papain in papain buffer (0.1 M sodium phosphate, 5 mM EDTA, 5 mM Cysteine-Hydrochloric acid, pH 6.5) for 72 h at 65°C in a heated shaker. Undigested remains were removed by centrifugation at 10,000 g for 10 min and supernatants (or middle layer when lipids were present) were collected and stored at 4°C until analysis. Primary isolate was used as a non-decellularized control. Papain solution without samples was incubated in parallel to use as a standard in the assays.

2.4 | DNA Quantification

The extent of decellularization was verified by DNA quantification. The amount of remaining DNA in papain-digested samples was measured using a Qubit fluorometer with dsDNA Kit (Q32850, Invitrogen) following the manufacturer's instructions. Individual samples were measured in triplicates, and DNA content was calculated as ng/mg of dried samples.

2.5 | Hydroxyproline Assay

A modified hydroxyproline assay [55] was used to determine the amount of collagen remaining after decellularization as the major ECM protein component. A hydroxyproline standard series (0.25 to 8 mg/mL) was prepared in papain solution and digested in parallel with the samples. After digestion, the samples and standards were diluted 1:10 in water. 100 μL 4 N NaOH was added to 100 μL of each dilution and autoclaved at 120°C and 15 psi above atmospheric pressure for 15 min to

hydrolyze the proteins. After allowing them to return to room temperature, the samples were neutralized by slowly adding 100 µL of 4 N hydrochloric acid (HCl). Chloramine-T solution (0.05 M Chloramine-T in 74% v/v H_2O, 26% v/v 2-propanol, 0.629 M NaOH, 0.140 M citric acid, 0.453 M sodium acetate, and 0.112 M acetic acid) was added, and samples were incubated for 20 min at room temperature. 625 µL Ehrlich's solution (1 M dimethylaminobenzaldehyde (DMAB) in 30% v/v HCl [conc. 32%] and 70% v/v 2-propanol) was added, and samples were incubated for 20 min in a 65°C water bath. After stopping the reaction in a cold-water bath, samples and standards were added in triplicates to a 96-well plate, and absorption was measured immediately at 560 nm using a plate reader. Absorption values from triplicates were averaged and corrected for background, and hydroxyproline content was calculated from the standards.

2.6 | Sulfated Glycosaminoglycan Content

Sulfated (S-) glycosaminoglycan content was measured as an estimate of total retained glycosaminoglycans as a major ECM component [56]. Sulfated glycosaminoglycan content in papain-digested samples was measured using the Blyscan sulfated glycosaminoglycan Assay Kit (Biocolor) according to the manufacturer's instructions.

2.7 | Total Protein Quantification

The total protein content of the DAT extracts was determined by a conventional bicinchoninic acid (BCA) assay kit (Pierce BCA Protein Assay Kit, Thermo Fisher Scientific) from pepsin-digested DAT samples. 1.25% DAT and bovine serum albumin standards in pepsin solution were diluted 1:20 in water and subjected to the assay according to the manufacturer's instructions.

2.8 | Hydrogel Preparation

For the generation of hydrogels, two different digestion methods were described in the referred protocols. Therefore, both methods were tested and compared for all DAT. The lyophilized DAT powders (12.5 mg/mL) were digested in 0.5 M acetic acid (AA) ("Voytik-Harbin method") [24] or 0.1 M HCl [52] with 1.25 mg/mL Pepsin (10 mg pepsin per 100 mg DAT) for 48 h at room temperature with slow rotation (1 rpm). Salt levels were adjusted by adding 10X DMEM or 10X DPBS and the pre-gel neutralized with 10 M/1 M NaOH, as indicated by phenol red. After neutralization, the solution was kept below 4°C to prevent premature gelation. Gelation could be induced by incubation at 37°C and occurred after ~15 min. A positive displacement pipette was required to evenly disperse the high-viscosity hydrogels. No $NaHCO_3$ was added to the 10X DMEM concentrate, as its reaction with AA seemed to interfere with gelation.

2.9 | Turbidity Measurement

Turbidity differences of pepsin-digested hydrogel samples were quantified by measuring absorption using a spectrophotometer (BioMate 3, Thermo Fisher Scientific). 1 mL of each hydrogel was transferred to a cuvette and absorption was measured at 860 nm.

2.10 | Rheological Characterization of Hydrogels

The viscosity of the seven hydrogels and collagen gel (control) was determined using a rotational oscillation-rheometer (Malvern Kinexus lab+m NETZSCH, Selb, Germany). The loading and the measurement were carried out at 15°C. The shear viscosity was measured using a 1° cone-plate geometry with a diameter of 40 mm for shear rates from 0.1 to 1000 s^{-1}, taking 10 measurement points per decade.

2.11 | Investigation of Hydrogel Printability

Bioprinting experiments were conducted on a microvalve-based 3D-bioprinting system (SuperFill-Custom, Black Drop Biodrucker GmbH, Aachen, Germany) with a microvalve diameter of 300 µm. The print head temperature was set to 5°C and varied between 10°C and 15°C. The print pressure was set to 0.2 bar to 1.5 bar depending on the hydrogel sample viscosity. Three cylinders with a diameter of 14 mm were selected as the printing model. Each of the cylinders was created in a droplet-based print, consisting of three layers placed on top of each other.

2.12 | Isolation of Primary Cells

The primary cells were processed strictly anonymously without recording patient-related data. The study was conducted in accordance with the Declaration of Helsinki and approved by the local ethics committee (Landesärztekammer Rheinland-Pfalz, No. 2021-15794_1).

2.12.1 | Isolation of Human Adipose-Derived Mesenchymal Stem Cells

Human adipose-derived mesenchymal stem cells (ASC) were derived from human adipose breast tissue samples from gynecological procedures (Department of Obstetrics and Gynecology, University Medical Center Mainz). The fresh tissue samples (~10–20 g) were transported in DMEM and immediately processed. The solid samples were washed twice in 70% ethanol and DPBS before transferring them to a plastic petri dish. The tissue was finely minced using sterile forceps and a surgical blade while removing any larger pieces of connective tissue or blood vessels. 10 mL of collagenase NB4 (1.5 U/mL in a buffer containing 66.7 mM NaCl, 6.7 mM KCl, 10 mM HEPES, 4.76 mM $CaCl_2$, pH 7.2) was added, the mixture transferred to a 50 mL conical tube and incubated for 1 h in a 37°C water bath, inverting the tube every 5 min. Digestion was stopped by adding 20 mL of fetal calf serum (FCS) containing culture medium (DMEM with high glucose, 10% FCS, and 1% penicillin/streptomycin solution), and the slurry was sieved through a 100 µm cell strainer to remove the remaining particles. After centrifugation (5 min, 400 g) the upper

fat layer and supernatant were removed. The pelleted cells were washed twice in DPBS, resuspended in 5 mL medium, and transferred to a T25 flask. The cells were incubated at 37°C and 5% CO_2 overnight. Non-adherent cell populations were removed by DPBS washes for the next 2 days. Cells were sub-cultured at 70% confluence and used until passage five for experiments. To induce adipogenic differentiation, ASC were cultured in induction medium consisting of DMEM culture medium containing 5% human platelet lysate (hPL) (HPCHXCRL10, PELO Biotech), supplemented with 1 μg/mL insulin (I9278, Sigma-Aldrich), 1 μM dexamethasone (D4902, Sigma-Aldrich), 500 μM 3-Isobutyl-1-methylxanthin (IBMX, I5879, Sigma-Aldrich), 1 μM rosiglitazone (R2408, Sigma-Aldrich) 33 μM biotin (B4639, Sigma-Aldrich) and 17 μM pantothenate (P5155, Sigma-Aldrich) for 14 days.

2.12.2 | Isolation of Human Dermal Microvascular Endothelial Cells

Human dermal microvascular endothelial cells (HDMEC) were isolated from juvenile foreskins (Department of Urology and Pediatric Urology, University Medical Center Mainz). Tissue samples were transported in DMEM supplemented with penicillin/streptomycin, kept at 4°C upon arrival and cells were isolated within 24 h. Cell isolation and cultivation were performed as described by Heller et al. [57].

2.12.3 | Isolation of Human Fibroblasts

Fibroblasts were isolated from human oral mucosa from biopsy samples (Department of Oral and Maxillofacial and Plastic Surgery, University Medical Center Mainz) by mechanical tissue processing [58]. DMEM (Sigma-Aldrich, St. Louis, MO, USA) supplemented with 10% Gibco FCS (Thermo Fisher Scientific, Waltham, MA, USA) and 100 U/100 mg/mL Penicillin/Streptomycin (Sigma-Aldrich, St. Louis, MO, USA) was used for fibroblast cultivation.

2.13 | Cellular Metabolic Activity Assay

Cellular metabolic activity of ASC and HDMEC on the hydrogels was assessed by an alamarBlue assay (DAL1025, Invitrogen) according to the manufacturer's instructions. 200 μL of neutralized hydrogels were plated in triplicates on 48 well plates and allowed to solidify for 15 min at 37°C. 2 mg/mL bovine collagen type I gels were prepared from a 5 mg/mL stock solution (500060635, Viscofan Bioengineering) by adding pre-chilled water, 10X DPBS, 1 M NaOH to adjust salt levels and to neutralize the acidic buffer. 200 μL of solution per well were plated in triplicates and allowed to solidify at 37°C for 15 min in an incubator.

For this assay, DAT from all isolation protocols was digested with 0.5 M AA or 0.1 M HCl, as previously described for hydrogel preparation. 200 μL of the two different neutralized hydrogels were plated in triplicates on 48-well plates and allowed to solidify. Alginate, known for poor support of both cell types was included as a negative control while collagen was included as a positive control [59]. Alginate gel discs were prepared by freezing 200 μL 1% sodium alginate solution with 10X DPBS adjusted salt levels for 30 min at −80°C. 200 μL 0.2 M $CaCl_2$ solution was added to the frozen alginate discs to induce crosslinking of the gels. After cross-linking, the gels were washed twice with DPBS including calcium before seeding the cells. ASC and HDMEC were seeded at a density of 20% (ASC: 4×10^3 cells/cm^2, HDMEC: 2×10^4 cells/cm^2) and allowed to attach and proliferate 48 h before conducting the experiments. For the alamarBlue assay, cell culture media were replaced by 200 μL medium containing 10% alamarBlue, and cells were incubated for 24 h. Fluorescence was measured using a plate reader (Ex: 525 nm, Em: 580–640 nm). For morphology assessment, cells were washed twice with DPBS and stained with 2 μM calcein AM (L3224, Invitrogen) in DPBS for 30 min. Hydrogels were then imaged using a fluorescence microscope (Leica, Germany) with a GFP/FITC filter set.

2.14 | In Vitro Differentiation of Human Adipose-Derived Mesenchymal Stem Cells

To assess the influence on differentiation, ASC were encapsulated in the different hydrogels and compared to collagen. Hydrogels were mixed with 9:1 with 10X ASC solution (2×10^7 cells/mL), resulting in final concentrations of 2×10^6 cells/mL. The collagen gel control was prepared as described before and the same number of cells was added. 150 μL of each cell/gel mix was plated on a 24-well plate in duplicates. One of each gel was cultured for 14 days with the induction medium containing 5% hPL. The cells were cultured as described before with medium changes every 2–3 days. The samples were imaged using bright field microscopy and stained with Oil Red O.

2.15 | Tube Formation Assay

The hydrogels were neutralized and 45 μL of the corresponding gel was pipetted in one well of an 8-well cell culture chamber on glass slides. Before sol–gel transition, 45,000 differentiated ASC and fibroblast at a final concentration of 2×10^6 cells/mL each were homogenized in the hydrogels. The hydrogels were then cured for at least 15 min at 37°C in an incubator. 100 μL triculture medium (PB-C-BH-895-0099-d, PELO Biotech) containing 5% hPL was added per well, and the cells were incubated overnight at 37°C. 4×10^4 HDMEC/100 μL triculture medium were added per well on the hydrogels. After 4 h, the cells were stained with calcein AM (1 μL calcein AM per well, 10 min), and the formation of first tubular networks was assessed microscopically.

2.16 | Statistical Analysis

Statistical analyses were performed using GraphPad Prism 8.4.3. Statistical significance of DAT characteristics (protein-, DNA-, hydroxyproline, and (s)-glycosaminoglycan content) in comparison to primary isolate was tested by repeated measure one-way ANOVA with Geisser–Greenhouse correction and Dunnett's correction for multiple comparisons of matched data (individual isolation rounds). Statistical differences in cellular

metabolic activity on hydrogels in comparison to collagen control were assessed by ordinary one-way ANOVA with Dunnett's correction for multiple comparisons.

3 | Results

3.1 | Manufacturing and Analyzing of Decellularized Adipose Tissue

Decellularized adipose tissue (DAT) extraction yielded a white material of similar weight and volume for all protocols (Figure 2A,B). DAT from protocols #4 and #5 had a granular, brittle structure while all other protocols resulted in fibrous materials. As a result, DAT from protocols #4 and #5 could be cryo-milled into a fine powder, while this was much more difficult with all other protocols. The apparent density, as estimated by the volume of samples of the same weight, was similar for most extracts, except for non-decellularized primary isolate and DAT #6, which had a much higher density in comparison (Figure 2A). The final yield after lyophilization in reference to the used amount of primary isolate (wet weight) was comparable for all protocols. Lyophilization of primary isolate without any further decellularization resulted in a yield of 43.2% ± 3.1% due to the high amount of retained fat. In accordance with the higher density, protocol #6 resulted in the second-highest yield of 16.3% ± 3.4%. Protocol #3 (7.5% ± 3.7%) and #4 (8.3% ± 1.2%) resulted in the lowest yield while protocol #1 (13.3% ± 2.7%), #2 (10.8% ± 1.9%), #5 (10.9% ± 0.3%), and #7 (12.0% ± 0.6%) yielded similar amounts of around 10% (Figure 2B). To minimize differences from density differences in later experiments, the protein content of the DAT materials was measured by a conventional BCA Assay to be able to normalize by total protein. The protein content was very similar for most samples with ~40% protein in reference to dry weight (#1: 38% ± 2%, #2: 38% ± 2%, #3: 38% ± 2%, #4: 41% ± 2%, #5: 44% ± 2%, #7: 40% ± 2%). In contrast, the higher-density samples showed a much lower content of 22% ± 1% (primary isolate) and 24% ± 3% (#6), respectively (Figure 2C).

The DAT samples were further characterized by measuring remaining DNA as an indication of decellularization, as well as hydroxyproline and glycosaminoglycan content to estimate the retention of ECM components.

In contrast to the protein content, the DNA content of the different DAT samples showed a higher variation (Figure 3A). The decellularization protocols #1 and #3 resulted in poor DNA reductions to 542 ± 256 and 301 ± 211 ng/mg dry weight of DAT, compared to 856 ± 119 ng/mg in the primary isolate (not

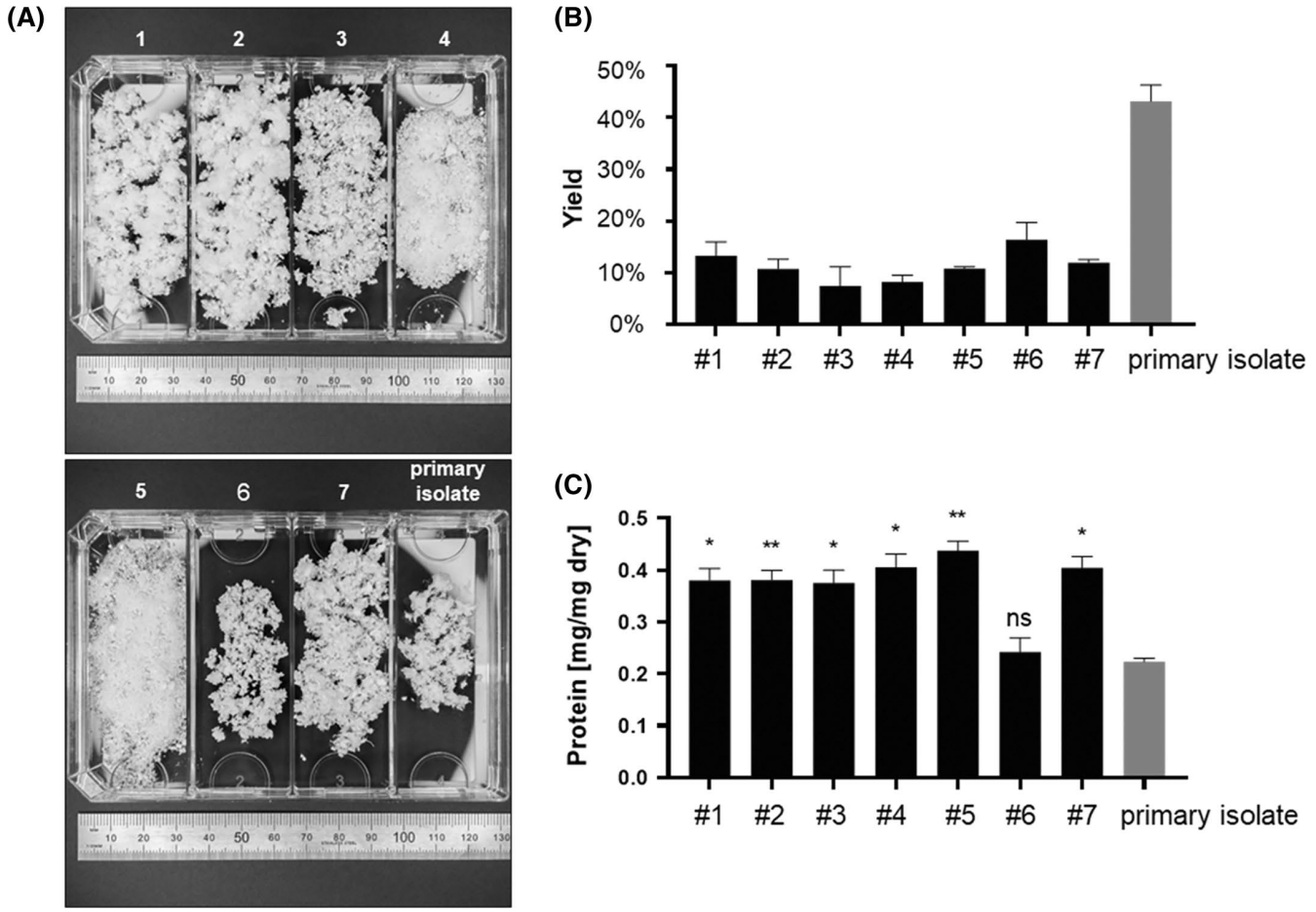

FIGURE 2 | Gross morphology and yield of decellularized adipose tissue (DAT) obtained from different protocols. (A) 200 mg of each DAT powder after lyophilization and milling. (B) Yield by weight after lyophilization (dry) in reference to the unprocessed primary isolate (wet). (C) Protein content of each sample was measured by BCA Assay. Data expressed as mean and standard deviation; $^{**}p < 0.01$; $^{*}p < 0.05$; not significant (ns) versus primary isolate; three individually sourced primary isolates were distributed across seven protocols for decellularization in three separate isolation rounds.

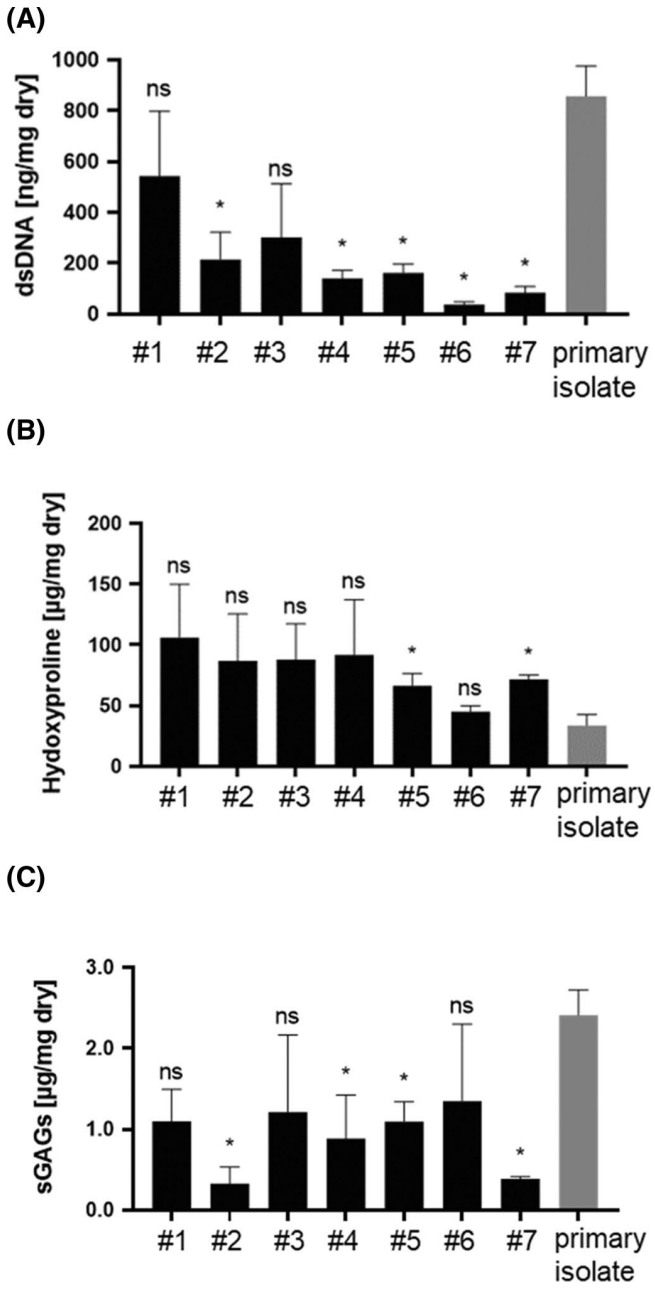

FIGURE 3 | Decellularized adipose tissue (DAT) characterization. (A) dsDNA content of DAT samples. (B) Hydroxyproline content of DAT samples. (C) sulfated glycosaminoglycan content of DAT samples. Data expressed as mean and standard deviation; *$p < 0.05$; not significant (ns) versus primary isolate; the experiments were carried out three times independently of each other with DAT samples from three different isolation rounds.

significant). The #4 and #5 protocols also resulted in similar levels of remaining DNA (#4140 ± 32; #5162 ± 34 ng/mg) while the lowest concentration was achieved by protocols #6 and #7 that includes a DNase digestion step (37 ± 11; 85 ± 23 ng/mg).

The hydroxyproline content as an estimate of collagen content reflected the protein concentration distribution, although with higher variability (Figure 3B). DAT #6 and primary isolate showed the lowest hydroxyproline concentration per mg dry (primary isolate: 33.6 ± 9.0 µg/mg dry; #6: 44.9 ± 5.0 µg/mg dry) while #1 (105.9 ± 44.1 µg/mg dry), #2 (86.9 ± 38.5 µg/mg dry), #3 (87.8 ± 29.5 µg/mg dry) and #4 (91.6 ± 45.7 µg/mg dry) all showed similar average hydroxyproline concentrations, with #5 (66.4 ± 10.1 µg/mg dry) and #7 (71.6.8 ± 3.6 µg/mg dry) extracts slightly lower.

In general, all isolation protocols reduced the glycosaminoglycan content compared to untreated primary isolate (2.41 ± 0.31 µg/mg) (Figure 3C), although with high variance between individual isolation runs. The lowest content of glycosaminoglycans was measured in DAT #7 (0.39 ± 0.03 µg/mg) and #2 (0.33 ± 0.20 µg/mg) samples, while the other samples showed values around 1 µg/mg (#1: 1.10 ± 0.39 µg/mg, #3: 1.21 ± 0.95 µg/mg; #4: 0.88 ± 0.54 µg/mg, #5: 1.09 ± 0.25 µg/mg, #6: 1.35 ± 0.95 µg/mg).

3.2 | Manufacturing and Analyzing of Decellularized Hydrogels

Even though not all protocols were developed to produce hydrogels in literature, all DAT samples could be solubilized into homogenous hydrogels by pepsin digestion with 0.5 M AA or 0.1 M HCl (Figures 4A and 5A). However, some differences in turbidity and grade of digestion were observed. Hydrogels from DAT #3 and #4 still contained some residual particles that could be removed by centrifugation. Otherwise, these hydrogels had a clear appearance, the same as hydrogels from DAT #2 and #7. The hydrogel from DAT #5 showed some slight turbidity, while hydrogels from DAT #1, #6, and the primary isolate were very turbid. This observation could be seen for hydrogels derived from digest with AA and HCl. The subjective appearance was verified by measuring the turbidity as absorption at 860 nm (Figures 4B and 5B).

A concentration of 1.25% (w/v) DAT in the hydrogels was the highest concentration possible, where all gels remained reasonably viscous and could still be mixed by slow inversion. The liquid hydrogel ("pre-gel", Figures 4C and 5C) could be turned into a solid gel by neutralization and incubation at 37°C (Figures 4D and 5D) for both variations of digest (AA and HCl). Hydrogels from the primary isolate and DAT #6 with 1.25% (w/v) DAT (digested with 0.5 M AA) did not solidify. Raising the concentration further was not possible for all gels as some turned so viscous that they could not be pipetted anymore. Therefore, the concentration of #6 and primary isolate gels was raised to 2.15% (w/v) DAT in subsequent experiments in an approximation of normalization by protein content. The resulting hydrogels showed pronounced differences in gel stability. While AA digested #1, #2, #3, and #7 hydrogels with 1.25% (~1.07% after neutralization) DAT were stable and easy to manipulate/transfer using forceps, #4, #5, #6 gels, and gels from primary isolate (the latter with adjusted gel concentrations) showed poor gel stability (Figure 4D).

HCl digested hydrogels #1, #2, #3, #5, and #7 were stable to manipulate and transfer. In contrast, hydrogels #4, #6, and the primary isolate formed no stable gel (Figure 5D). To address concerns regarding possible contamination due to the semi-sterile isolation process, the gels were incubated with a standard culture medium for an extended period of time. After 4 weeks of incubation under standard cell culture conditions, no

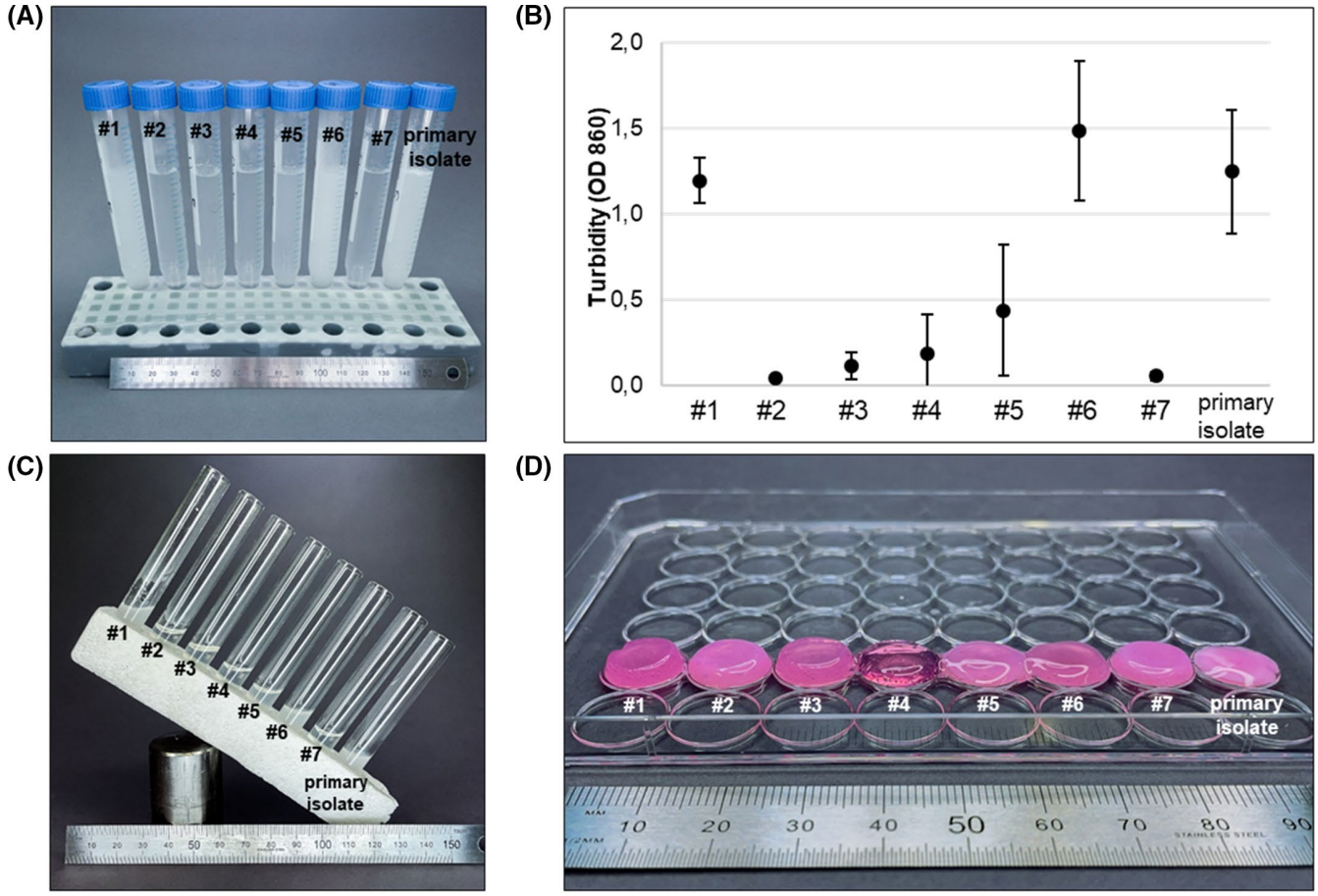

FIGURE 4 | Decellularized adipose tissue hydrogels, digested using AA. (A) Pepsin digestion (0.5 M AA) of DAT resulted in hydrogels of varying turbidity. (B) Quantification of turbidity by absorption at 860 nm. Data expressed as mean and standard deviation; the experiment was carried out three times independently of each other with DAT samples from three different isolation rounds. (C) Hydrogels remained liquid after digestion and (D) formed semi- solid gels after neutralization and 15 min incubation at 37°C.

contamination could be detected microscopically or by medium color change (not shown).

3.3 | Cellular Metabolic Activity and Morphology on Hydrogels

The cellular response to the hydrogels is the most important criterion to assess their suitability for tissue engineering. The hydrogels were assessed for their support of HDMEC and ASC metabolic activity in monoculture by an alamarBlue assay and compared to collagen as positive control and alginate as negative control [59, 60]. All samples were normalized to collagen as 100% cellular metabolic activity. In addition, the influence of the concentration of the used acids for pepsin digest while hydrogel preparation on the metabolic activity of HDMEC and ASC was tested. For both cell types, ASC and HDMEC, the use of HCl instead of AA or digestion showed a positive effect on the metabolic activity of the cells (Figure 6).

The metabolic activity of ASC on hydrogels was generally lower than that of HDMEC and lower in comparison to collagen (positive control). The ASC showed an increased metabolic activity with the replacement of 0.5 M AA to 0.1 M HCl on all hydrogels (Figure 6A). The use of 0.1 M HCl for digestion has the highest benefit for ASC metabolic activity, especially for hydrogel #2. For hydrogel #6, the data is to be considered with reservations, since with this concentration of HCl, no stable hydrogel was formed.

The hydrogel generated from the #2 protocol supported ASC almost as good as collagen (81% ± 12%) when 0.1 M HCl was used. #1, #3, #4, #5 and #7 hydrogels resulted in a comparable cellular metabolic activity of 50% ± 17%, 47% ± 4%, 49% ± 12%, 48% ± 4% and 48% ± 5% with the use of 0.1 M HCl. 0.5 M AA led to results comparable to alginate (negative control) (15% ± 7%) (Figure 6A).

The metabolic activity of HDMEC showed similar effects to the ASC (Figure 6B). For all hydrogels, the digest with 0.1 M HCl led to the highest cellular metabolic activity with #1 (143% ± 16%), #2 (139% ± 22%), #3 (140% ± 24%), #4 (146% ± 36%), #5 (125% ± 14%), #6 (152% ± 5%) and #7 (135% ± 23%). For hydrogel #6, again, the data is to be considered with reservations since with this concentration of HCl no stable hydrogel was formed. 0.5 M AA led to the lowest cellular metabolic activity, especially for hydrogel #4 (15% ± 5%) and #7 (20% ± 1%).

Calcein staining was used to compare cellular morphology on the different hydrogels. Analyses of cell morphology on a cell

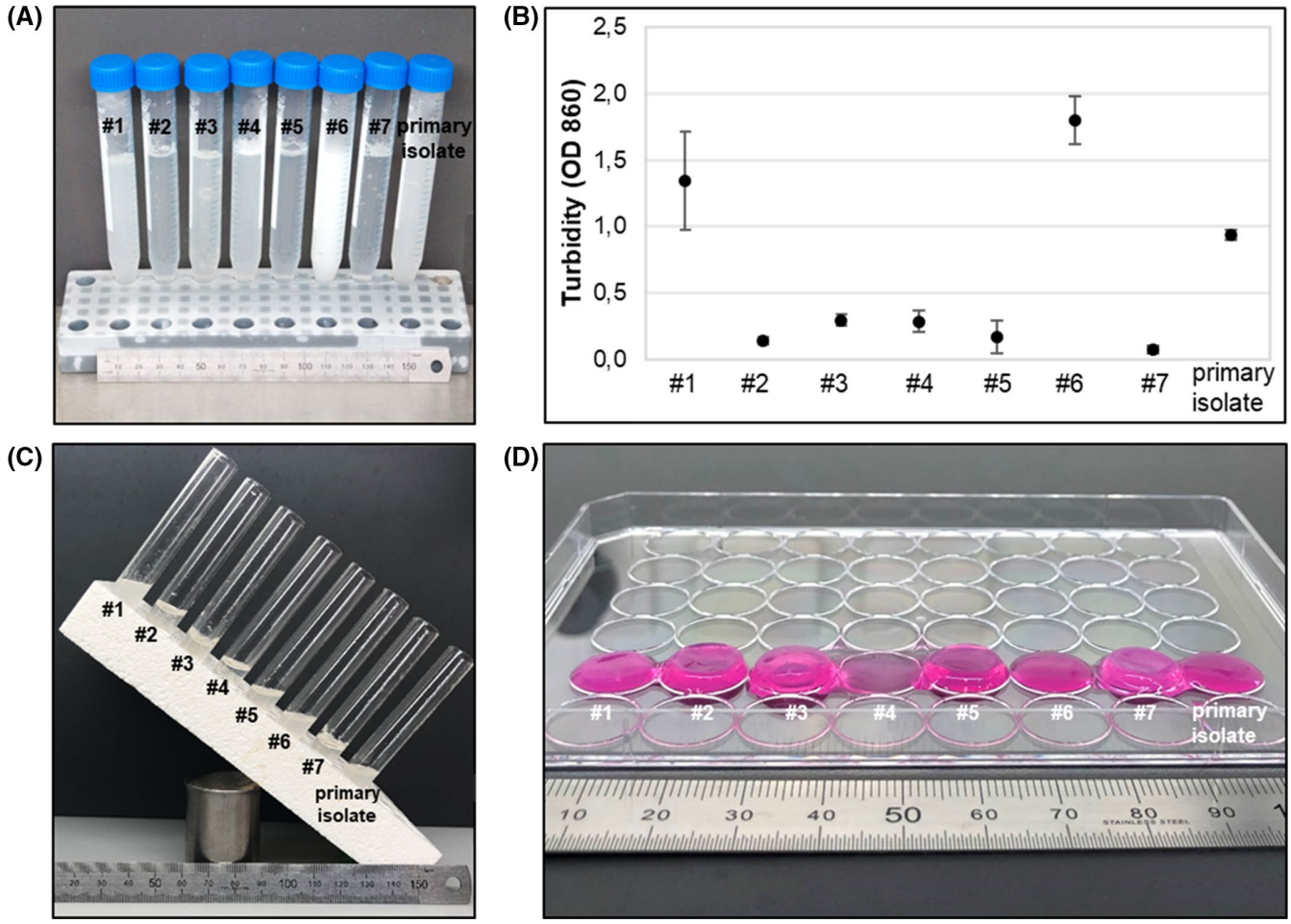

FIGURE 5 | Decellularized adipose tissue hydrogels, digested using HCl. (A) Pepsin digestion (0.1 M HCl) of DAT resulted in hydrogels of varying turbidity. (B) Quantification of turbidity by absorption at 860 nm. Data expressed as mean and standard deviation; the experiment was carried out three times independently of each other with DAT samples from three different isolation rounds. (C) Hydrogels remained liquid after digestion and (D) formed semi-solid gels after neutralization and 15 min incubation at 37°C.

culture plate and on collagen were used as positive controls. The primary isolate was not included since it was too unstable and did not withstand the medium changes.

Calcein stains generally confirmed the results of the cellular metabolic activity experiments. Hydrogels #4, #5, and #6 digested with AA had a lower number of calcein stained and thus living ASC. In hydrogels #1, #2, #3, and #7 digested with AA ASC showed similar cell number and cell morphology as in the collagen positive control (Figure 7A). In comparison, ACS on all hydrogels #1 - #7 digested with HCl were very viable (Figure 7B).

HDMEC did not tolerate #4 and #5 hydrogels which were digested with 0.5 M AA and did not spread on the gel, with only very few cells visible. However, the cells did attach and survived on #1, #2, #3, and #7 hydrogels and, to a lesser extent, on the #6 hydrogel (Figure 8A). In comparison, HDMEC on all hydrogels #1–#7 digested with HCl were viable. The highest cell survival of HDMEC was seen on hydrogels #2 and #3. The cells were also viable on hydrogels #1, #5, #6, and #7 (in some samples, difficult to recognize, as the hydrogels tended to be self-fluorescent). The weakest survival of HDMEC was observed on hydrogel #4, although it was higher than on the hydrogels digested with AA (Figure 8B).

3.4 | Differentiation of Adipose-Derived Mesenchymal Stem Cells on Hydrogels

To assess the benefit of hydrogels for adipocyte differentiation, cells were seeded on hydrogels and subjected to DMEM/hPL-based differentiation medium (Figure 9) for 14 days. The cells were imaged Oil Red O stained using a bright field microscope. On collagen as a positive control, just like on the various hydrogels, ASC differentiated detectably. The highest lipid accumulation could be seen in cells cultured on collagen and, to a lesser extent in cells cultured on all hydrogels. For hydrogel #6 and #7 digested with AA (Figure 9A) and hydrogel #3, #5, and #7 digested with HCl (Figure 9B), only small lipid droplets could be observed, but were clearly visible at higher magnifications of objective lens.

3.5 | Rheological Characterization of Hydrogels for 3D-Bioprinting

The viscosity and 3D-printability of the various hydrogels digested with HCl were analyzed to ensure their usability as a material in 3D-bioprinting.

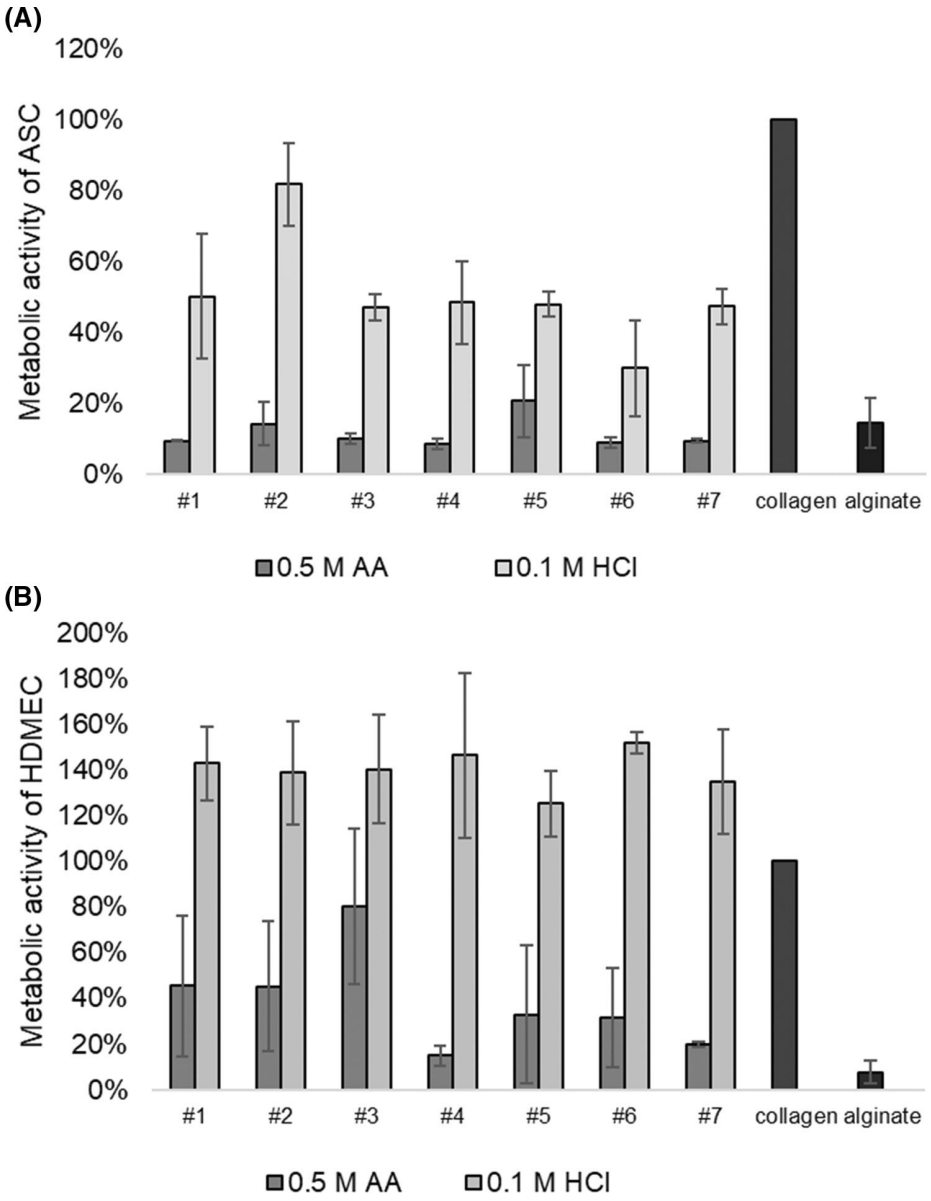

FIGURE 6 | Metabolic activity of ASC (A) and HDMEC (B) on hydrogels after 2 days. For preparation of hydrogels, DAT #1 - #7 was digested with two different acids. For AA the concentration of 0.5 M was used; HCl was tested in the concentration of 0.1 M. Cellular metabolic activity is expressed in reference to collagen as positive control. Alginate was used as a negative control. The experiments were carried out three times independently with cells from different donors.

The viscosity was measured as a function of the shear rate. All hydrogels, as well as the collagen control, showed a decrease in viscosity with increasing shear rate, which can be described as approximately linear for the hydrogels. Collagen shows an initially steep, then flatter decreasing curve with increasing shear rate. The different hydrogels have different viscosities. They can be listed from highest viscosity to lowest viscosity as follows: #1 > #3 > #2 > #7 > 4# > 5# > 6# > collagen (Figure 10).

To test the printability, the hydrogels were printed as cylinders consisting of three layers. To assess the stability, the inner diameter of the cylinders was measured. The more unstable a cylinder and, therefore, a hydrogel is, the more the shape runs, and the inner diameter is reduced compared to the initial value of 14 mm.

The hydrogels were ejected through the nozzle of the printer using compressed air. Especially hydrogels previously determined to be more viscous were found to be segregated during printing. This manifested itself in the fact that parts of the liquid phase were pressed out of the sol–gel, while parts of the DAT fibrils remained adhered to the valve internals. With the less viscous hydrogels, this behavior was much less pronounced, and from which it can be assumed that the composition of the gel changed only minimally, if at all. This observation was also reflected in the fact that the actual hydrogels did not harden completely even after incubation at 37°C. Instead, they retained their watery consistency. Therefore, the result of the pressure test must be viewed with caution. Hydrogel #4 was printable into the most stable cylinders. Compared to the cylinders of the other hydrogels and the collagen control, the rings were significantly thinner, and after curing the printed cylinders clearly

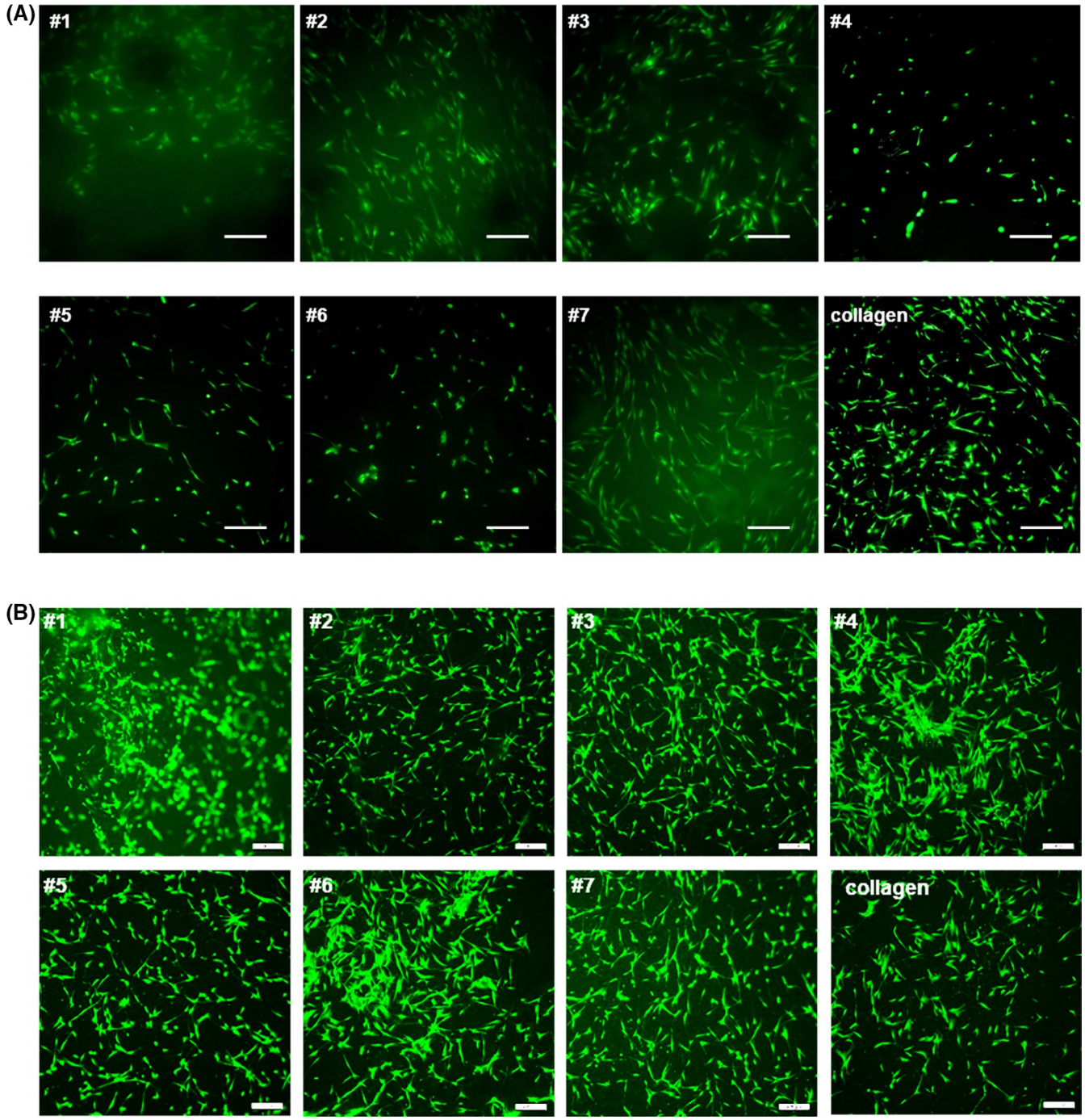

FIGURE 7 | ASC (4×10^3/mm^2) were seeded on different hydrogels #1–#7 and collagen as positive control and were cultivated for 48 h. (A) Hydrogels #1–#7 digested with AA (0.5 M) or (B) hydrogels digested with HCl (0.1 M). The experiments were carried out three times independently with cells from different donors. Scale Bar = 200 μm.

showed a stable shape. For the cylinders of hydrogels #3, #5, #6, and #7, the surface of the structure showed wavy extensions, which can be attributed to the individually printed dots. This was also observed for the collagen control in an attenuated form. All four gels could be cured by incubation into a mostly solid gel. In the case of hydrogels #1 and #2, the pressure resulted in strongly flowing cylinders with a largely smooth shape. Since both gels also did not solidify after incubation at 37°C, it can be assumed that only the aqueous component of the hydrogel could be printed, particularly in the case of these hydrogels (Figure 11A).

The visual impressions of the cylinders were confirmed by measuring the inner diameters of the printed cylinders (Figure 11B). The cylinders of hydrogel #4 had the largest inner diameter (11.42 ± 0.15 mm). This confirmed the assumption that the most stable cylinders could be printed with hydrogel #4, which had the least warping due to their dimensional stability. The cylinders of hydrogels #3 (10.53 ± 0.31 mm), #6 (10.97 ± 0.51 mm) and #7 (10.88 ± 0.59 mm) confirmed the moderate stability of the printed cylinders, while the printing of hydrogels #1 (9.75 ± 0.09 mm), #2 (9.84 ± 0.12 mm) and the collagen control (9.93 ± 0.09 mm) led to a significantly smaller inner diameter (Figure 11B).

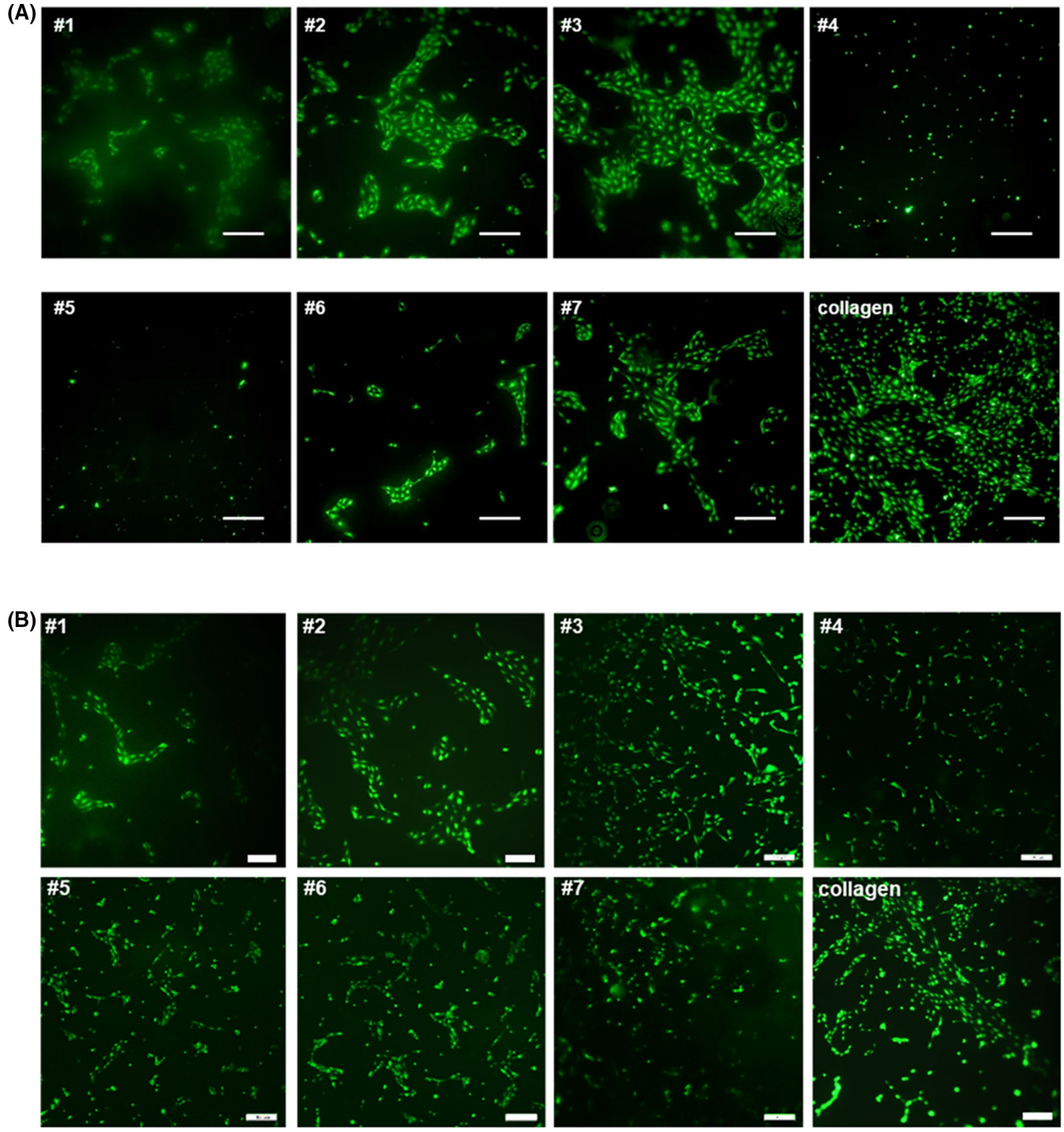

FIGURE 8 | HDMEC (2×10^3/mm^2) were cultured for 48 h on hydrogels #1–#7 or collagen as positive control. (A) Hydrogels digested with AA (0.5 M) or (B) hydrogels digested with HCl (0.1 M). The experiments were carried out three times independently with cells from different donors. Scale Bar = 200 μm.

3.6 | Endothelial Vascularization on Hydrogels as Triculture

The hydrogels used for the tube formation assay represent a triculture with ASC, fibroblasts, and endothelial cells. The ASC and fibroblasts were added to the hydrogels, and the endothelial cells were seeded on top. The assessment of tubes that are formed serves to evaluate the possible vascularization in the triculture system in the hydrogels. More and better-defined tubes were formed on all hydrogels #1–#7 than on collagen as positive control. The formation of first tubular networks is weakest on hydrogel #5 compared to the remaining samples (Figure 12).

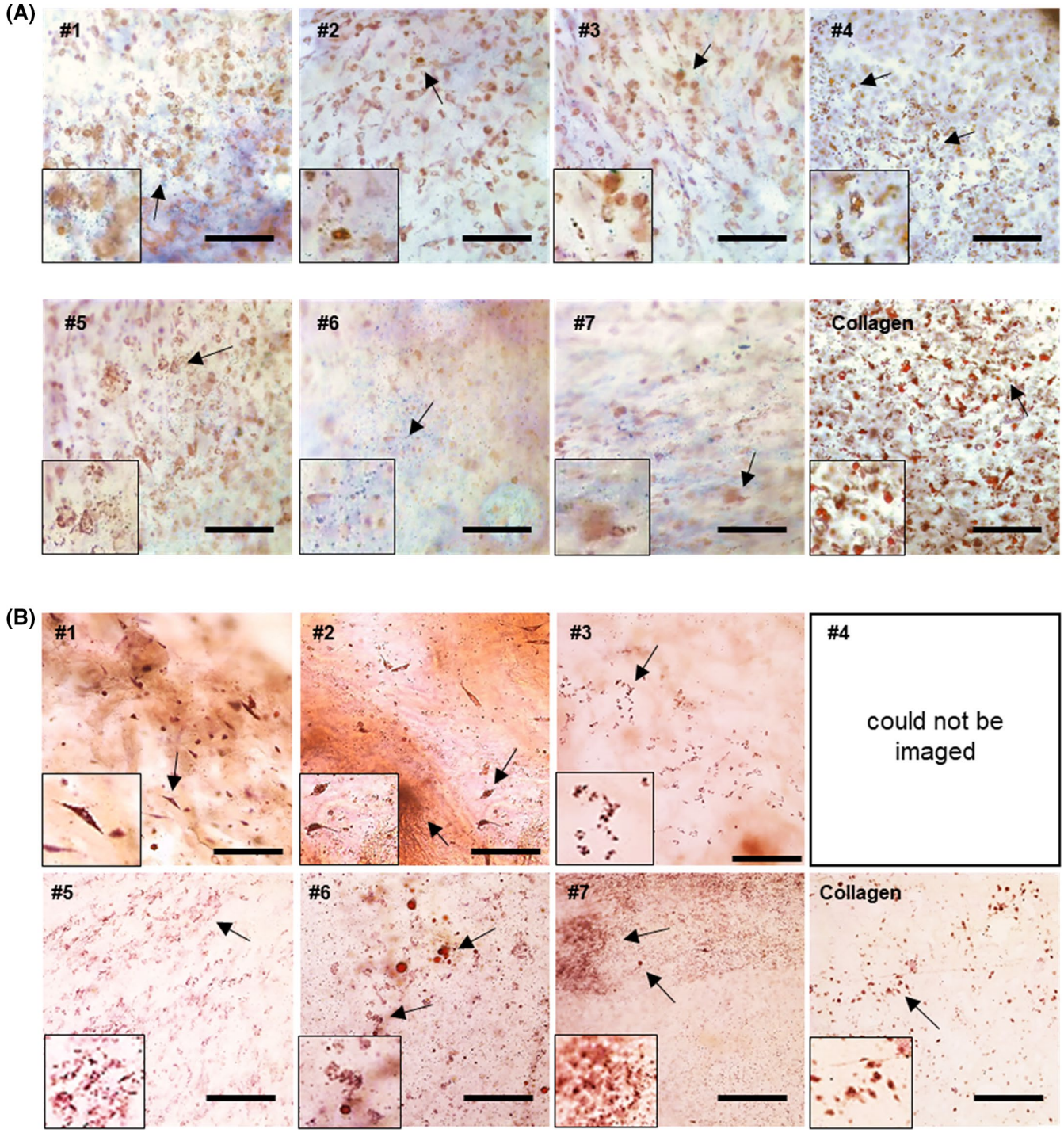

FIGURE 9 | ASC differentiation (2×10^6 cells/ml) on hydrogels #1–#7 digested with (A) 0.5 M AA and (B) 0.1 M HCl as well as on collagen as positive control. ASC were cultivated for 14 days. The hydrogel #4 digested with 0.1 M HCl could not be imaged due to insufficient stability of the gel. The cell differentiation was detected by Oil Red O staining of lipid droplets. Arrows point to the lipid droplets. The experiments were carried out three times independently with cells from different donors. Scale Bar = 200 μm.

4 | Discussion

To generate hydrogels suitable for adipose tissue engineering, decellularized adipose tissue (DAT) was produced from porcine adipose tissue using seven different protocols. There were noticeable differences in the production of DAT depending on the protocol. The DAT differed on the one hand in their consistency and turbidity and on the other hand in their DNA content and the content of ECM components. A high level of residual DNA in the DAT is a sign of incomplete decellularization of the porcine fat samples [27]. The DAT samples of protocols #1 and #3 showed a comparatively high residual DNA content. This leads to the conclusion that these two are less suitable for further utilization as scaffolds for tissue engineering than the other DAT samples. Since these two protocols use Triton-X100, it can be assumed that poorer DNA removal is

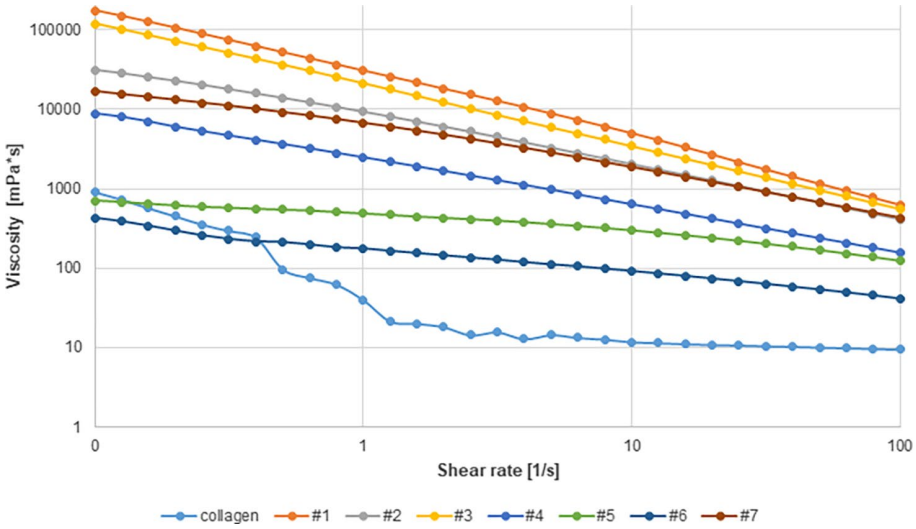

FIGURE 10 | Viscosity of the various hydrogels digested with 0.1 M HCl. The viscosity in mPa×s is plotted against the shear rate in s^{-1} used in the examination. The viscosity of the seven different hydrogels (#1–#7) and collagen as control are shown. The experiment was carried out once.

achieved with this detergent. In comparison to this, the use of SDS or additional DNAse treatments, utilized for the other hydrogels, led to a more efficient DNA removal. Standards for safe levels of residual DNA in the hydrogels from the ECM still need to be determined. This is an aspect that needs to be considered in further experiments when using hydrogels that have residual DNA.

When decellularizing porcine fat samples, it is important to preserve the ECM components so that the resulting scaffold is as close as possible to the physiological ECM of adipose tissue in its composition. Thus, the highest possible levels of hydroxyproline and glycosaminoglycans (GAGs) indicate good preservation of the ECM components in the DAT samples. While the use of SDS has a positive effect on DNA removal, the detergent seems to have a negative effect on the hydroxyproline content. In particular protocols #5 and #6, which include SDS treatment, show a reduced hydroxyproline content. The use of triton-X100 appears to have less of an effect on hydroxyproline. The content of GAGs varies strongly between the individual protocols. It should be mentioned that the analysis of the content of GAGs could be influenced by residual reagents in the decellularization process [61]. Residual reagents should be largely avoided by proper washing steps at the end of the decellularization process.

Hydrogels were generated from the different DAT samples. Since this method is described in literature in some protocols with AA and in other protocols with HCl for the digestion of DAT, we discuss the comparison between the use of these two acids. Reference was made to the most commonly used acid solutions for the preparation of ECM hydrogels, including 0.5 M AA (Voytik-Harbin method) [62] and 0.1 M HCl (Freytes method) [63]. There were clear differences depending on whether the DAT was digested with AA or HCl. In particular, the compatibility of the hydrogels with the cells that were used showed that the metabolic activity of ASC and HDMEC were better on hydrogels digested with HCl. The results of the analysis of adipocyte differentiation must be related to their respective collagen control and cannot simply be compared between the gels with AA or HCl digestion. This is because the experiments took place at different times with different cell donors. This resulted in different appearances of the respective collagen controls. Therefore, these results must be considered with reservations. The key message of the result is that adipocyte differentiation is possible on all hydrogels. The poorer metabolic activity of the cells on hydrogels prepared with AA could be due to the hyperosmotic state within the hydrogel. While gels digested with HCl could be adjusted to a physiological osmolarity by neutralization, it was shown that the osmolarity of 0.5 M AA could not be reduced to a physiological state [64]. Since increased osmolar stress can lead to numerous disturbances within the cells due to the hypertonic effect, the reduced metabolic activity of the cells on the AA hydrogels can probably be explained by the non-optimal conditions within the hydrogel [65].

The handling of the hydrogels revealed clear differences in the stability and printability of the hydrogels. Pouring of the hydrogels and a viscosity measurement confirmed these observations and showed that DAT #1, #2, #3, and #7 could be converted to dimensionally stable hydrogels, while the hydrogels from DAT #4, #5, and #6 resulted in more unstable hydrogels. The 3D printing of the hydrogels into cylindrical molds contradictorily demonstrated that the hydrogels #4, #6, and #7 allowed the stable formation of cylinders and that the printed cylinders out of hydrogel #1, #2, #3, and #5 did not. However, this result must be viewed critically because the hydrogels dissolved into their components during the printing process. This can presumably be attributed to the fact that the gels with higher collagen content tended to deposit fibrils on the inside of the valve (e.g., corresponding spring elements). This led to a phase separation in which only the aqueous solution was pressed through the valve, while the fibrous collagen components remained in the valve. It can be recommended to either use a different bioprinting modality (e.g., microextrusion instead of drop-on-demand) or to switch to a hybrid printing/casting process.

The appropriate tissue engineering material should have sufficient stability to hold the manufactured tissue together and withstand the transplantation process, but at the same time,

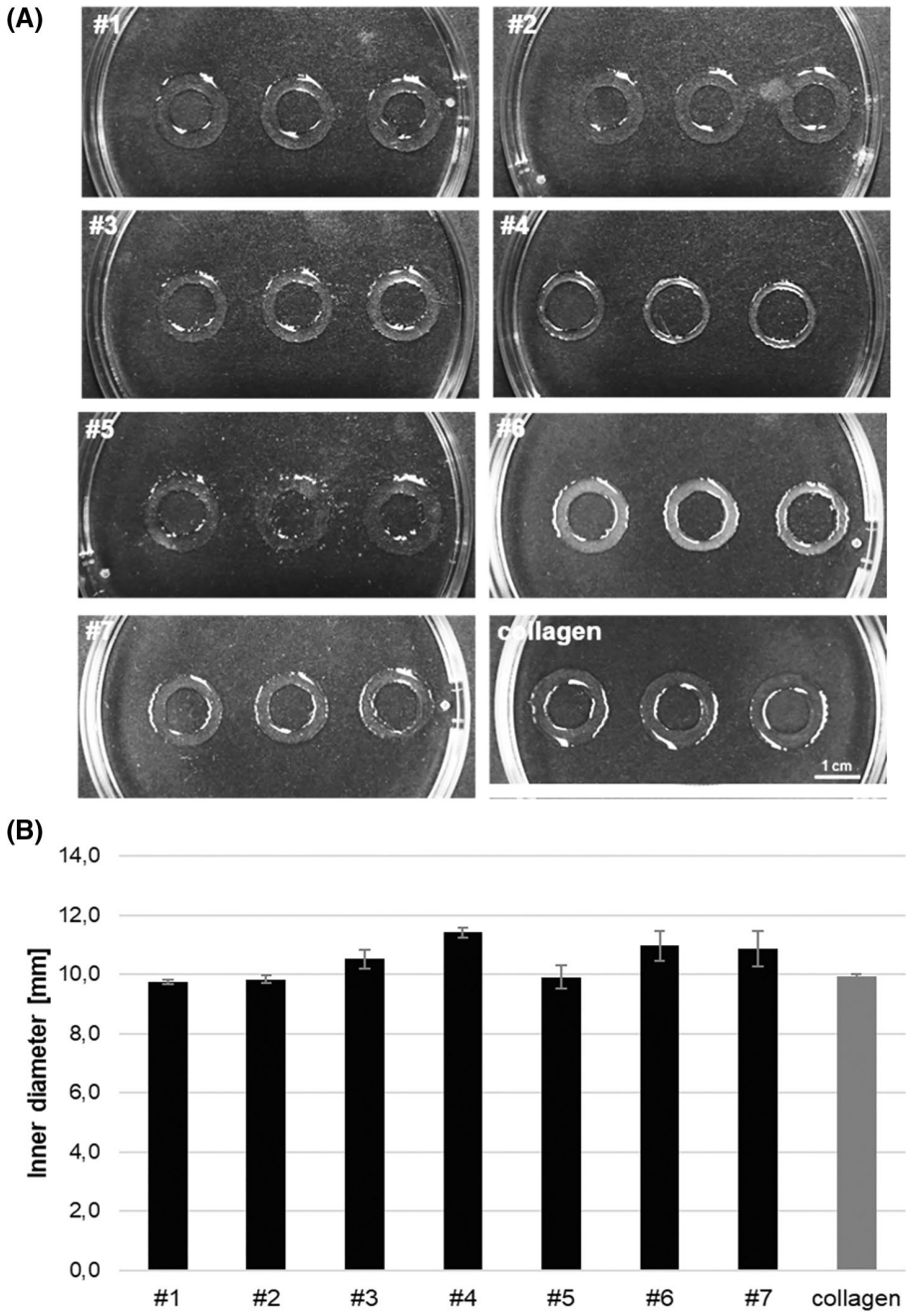

FIGURE 11 | 3D-printability of the various hydrogels digested with 0.1 M HCl. (A) For each hydrogel (#1–#7) and collagen control, three cylinders consisting of three layers upwards were printed. A scale of 1 cm is displayed. (B) The inner diameter of the cylinders was determined and presented graphically. The experiment was carried out once in a triplet.

ensure sufficient flexibility to allow the cellular components to proliferate, differentiate and also support angiogenesis. The results lead to the conclusion that the mechanical properties of the hydrogels are significantly influenced by the decellularization method used. The protocols tested differ, for example in the choice of detergents used. Protocols #1, #2 and #3 use Triton-X100 for decellularization, while protocols #4, #5, and #6 use SDS. The choice of detergent can influence the stability of the resulting hydrogel. The use of SDS can lead to the degradation of collagen from the ECM [66]. The stiff properties of collagen fibers contribute to the shape stability of the ECM [67]. The influence of the decellularization method on the collagen content in the respective DAT or hydrogels can be assumed from the hydroxyproline content [68]. Therefore, SDS-induced degradation of collagen fibers in the DAT hydrogels could explain the reduced stability of hydrogels #4, #5, and #6, while the use of Triton-X100 and physical methods for decellularization did not lead to increased degradation of collagen fibers and thus stability is not as severely affected [29].

The compatibility of the hydrogels with ASC and HDMEC, as important cellular components, is crucial for the successful generation of adipose tissue equivalents. For both ASC and HDMEC, the use of HCl in hydrogel production resulted in improved cellular metabolic activity compared to AA. A comparison of the hydrogels digested with HCl showed that the metabolic activity and

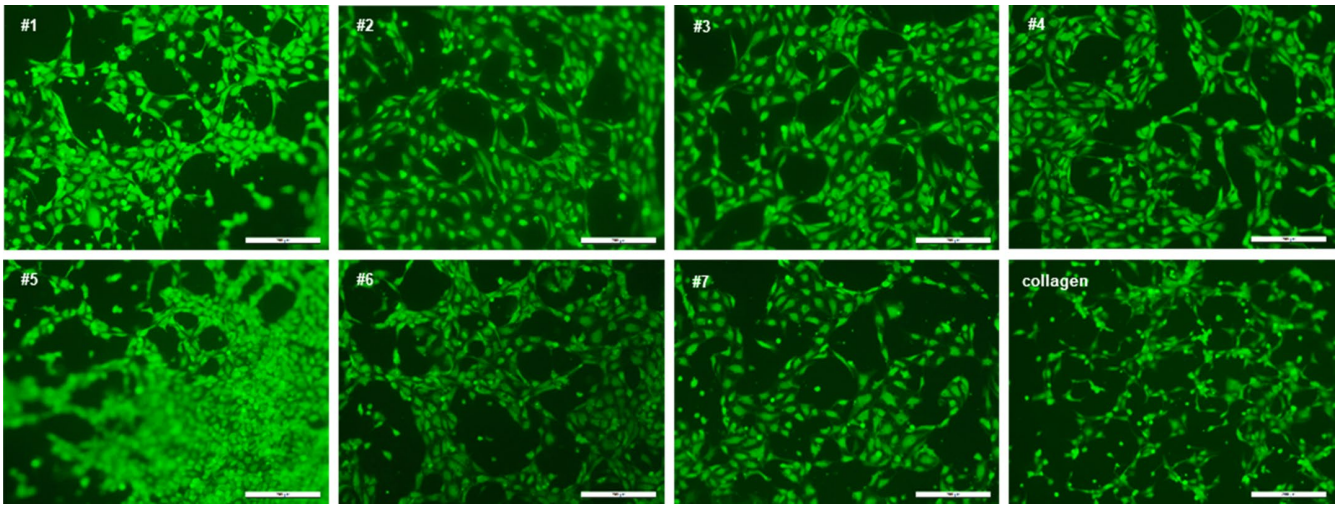

FIGURE 12 | Formation of first tubular networks of human dermal microvascular cells after 4 h on the various hydrogels #1–#7 digested with 0.1 M HCl. Collagen was used as a positive control. The gels contained ASC and fibroblasts, while endothelial cells were seeded on top (triculture model). The endothelial cells were visualized with calcein staining. Scale Bar = 200 μm. The experiment was carried out three times independently with cells from different donors.

morphology of the ASC and HDMEC were most pronounced on hydrogel #2. A possible reason for the differences in cellular metabolic activity and morphology lies in the different effects of the decellularization detergents used, such as SDS, and thus the cytocompatibility of the hydrogels. The differentiation of the ASC has taken place on all hydrogels. It has already been described in various publications that hydrogels from DAT support adipogenic differentiation in vitro [36, 38, 69]. The differences that occurred between the hydrogels tested may be due to numerous factors. An important factor in the differentiation of ASC to adipocytes is the presence of growth and differentiation factors within the hydrogel structure [70]. The use of SDS can significantly reduce the growth factor content of the ECM and the ability of the ECM to support in vitro cell growth. The use of trypsin or Triton-X100 also results in a reduction in growth factors, but to a lesser extent, and factors such as basic fibroblast growth factor (bFGF) are largely retained, resulting in better support for cell growth [71].

Finally, the angiogenesis-promoting effect of the hydrogels was investigated using a tube formation assay. The formation of beginning tubular networks of endothelial cells was shown on all hydrogels, even better than on the collagen positive control. This effect could be due to the remnants of angiogenic growth factors in the native ECM, which are not present in pure collagen. If so, this effect appears to be less sensitive than ASC differentiation in terms of the amount of growth factors, as there was no difference between the formation of the tubular networks on the hydrogels treated with SDS or with Triton-X-100 during preparation.

5 | Conclusions

We showed that different approaches for decellularization of adipose tissue and subsequent acid digestion have significant effects on the production of a suitable scaffold for adipose tissue reconstruction. In our work, hydrogel #2 [52] digested with HCl proved to be the best option for scaffold generation, as the production of decellularized ECM worked efficiently, allowing to produce hydrogels that are very cell-compatible, promote cellular metabolic activity, and promote ASC differentiation as well as endothelial cell vascularization. The use of Triton-X100 in combination with physical methods for decellularization led to significant DNA removal. At the same time, the detergent has a positive effect on the preservation of hydroxyproline and, thus, ECM components such as collagen and on compatibility with cells. The tested hydrogel is, therefore, suitable for a wide range of procedures within the tissue engineering of vascularized fatty tissue. The hydrogel of the second choice is #7 digested with HCl. The method avoids the use of detergents and is based on physical decellularization steps, which also led to an efficient decellularization of the DAT. Additionally, the use of DNase resulted in the effective removal of DNA residues. The resulting hydrogel was cell-compatible and promoted the analyzed cellular properties. The drop-based bioprinting method carried out on the hydrogels did not allow a definitive statement on the printability of the hydrogel. To get a better impression, further 3D printing trials must follow. The generation of an in vitro prevascularized fatty tissue equivalent could largely replace conventional breast reconstruction strategies such as silicone implants or autologous fat transplants. By using autologous cells, an immunological reaction to the inserted implant should be avoided as far as possible, and at the same time, optimal integration of the implant should be made possible through its similarity to physiological tissue.

Acknowledgments

We thank the Core facility of Cell Biology Unit for technical support.

Ethics Statement

The study was conducted in accordance with the Declaration of Helsinki and approved by the local ethics committee (Landesärztekammer Rheinland-Pfalz, No. 2021-15794_1).

Consent

Informed consent was obtained from each patient. The primary cells were processed strictly anonymously without recording patient-related data.

Conflicts of Interest

The authors declare no conflicts of interest.

Data Availability Statement

All data can be requested from the corresponding author.

References

1. C. M. Mahoney, C. Imbarlina, C. C. Yates, and K. G. Marra, "Current Therapeutic Strategies for Adipose Tissue Defects/Repair Using Engineered Biomaterials and Biomolecule Formulations," *Frontiers in Pharmacology* 9 (2018): 507, https://doi.org/10.3389/fphar.2018.00507.

2. T. J. Puls, C. S. Fisher, A. Cox, et al., "Regenerative Tissue Filler for Breast Conserving Surgery and Other Soft Tissue Restoration and Reconstruction Needs," *Scientific Reports* 11, no. 1 (2021): 2711, https://doi.org/10.1038/s41598-021-81771-x.

3. D. Schmauss, H.-G. Machens, and Y. Harder, "Breast Reconstruction After Mastectomy," *Frontiers in Surgery* 2 (2015): 71, https://doi.org/10.3389/fsurg.2015.00071.

4. J.-W. Groen, V. L. Negenborn, J. W. R. Twisk, J. C. F. Ket, M. G. Mullender, and J. M. Smit, "Autologous Fat Grafting in Cosmetic Breast Augmentation: A Systematic Review on Radiological Safety, Complications, Volume Retention, and Patient/Surgeon Satisfaction," *Aesthetic Surgery Journal* 36, no. 9 (2016): 993–1007, https://doi.org/10.1093/asj/sjw105.

5. T. Mashiko and K. Yoshimura, "How does fat survive and remodel after grafting?," *Clinics in Plastic Surgery* 42, no. 2 (2015): 181–190, https://doi.org/10.1016/j.cps.2014.12.008.

6. H. Karagoz, F. Zor, E. Goktas, and V. S. Gorantla, "Adipogenesis for Soft Tissue Reconstruction," *Current Opinion in Organ Transplantation* 24, no. 5 (2019): 598–603, https://doi.org/10.1097/MOT.0000000000000694.

7. C. Conci, L. Bennati, C. Bregoli, et al., "Tissue Engineering and Regenerative Medicine Strategies for the Female Breast," *Journal of Tissue Engineering and Regenerative Medicine* 14, no. 2 (2020): 369–387, https://doi.org/10.1002/term.2999.

8. E. Donnely, M. Griffin, and P. E. Butler, "Breast Reconstruction With a Tissue Engineering and Regenerative Medicine Approach (Systematic Review)," *Annals of Biomedical Engineering* 48, no. 1 (2020): 9–25, https://doi.org/10.1007/s10439-019-02373-3.

9. L. Bacakova, J. Zarubova, M. Travnickova, et al., "Stem Cells: Their Source, Potency and Use in Regenerative Therapies With Focus on Adipose-Derived Stem Cells - A Review," *Biotechnology Advances* 36, no. 4 (2018): 1111–1126, https://doi.org/10.1016/j.biotechadv.2018.03.011.

10. M. A. Banani, M. Rahmatullah, N. Farhan, et al., "Adipose Tissue-Derived Mesenchymal Stem Cells for Breast Tissue Regeneration," *Regenerative Medicine* 16, no. 1 (2021): 47–70, https://doi.org/10.2217/rme-2020-0045.

11. N. K. Dubey, V. K. Mishra, R. Dubey, Y.-H. Deng, F.-C. Tsai, and W.-P. Deng, "Revisiting the Advances in Isolation, Characterization and Secretome of Adipose-Derived Stromal/Stem Cells," *International Journal of Molecular Sciences* 19, no. 8 (2018): 2200, https://doi.org/10.3390/ijms19082200.

12. S. Rautiainen, T. Laaksonen, and R. Koivuniemi, "Angiogenic Effects and Crosstalk of Adipose-Derived Mesenchymal Stem/Stromal Cells and Their Extracellular Vesicles With Endothelial Cells," *International Journal of Molecular Sciences* 22, no. 19 (2021): 10890, https://doi.org/10.3390/ijms221910890.

13. A.-C. Volz, B. Huber, and P. J. Kluger, "Adipose-Derived Stem Cell Differentiation as a Basic Tool for Vascularized Adipose Tissue Engineering," *Differentiation; Research in Biological Diversity* 92, no. 1–2 (2016): 52–64, https://doi.org/10.1016/j.diff.2016.02.003.

14. N. Zeng, H. Chen, Y. Wu, and Z. Liu, "Adipose Stem Cell-Based Treatments for Wound Healing," *Frontiers in Cell and Developmental Biology* 9 (2021): 821652, https://doi.org/10.3389/fcell.2021.821652.

15. M. J. Bissell and J. Aggeler, "Dynamic Reciprocity: How Do Extracellular Matrix and Hormones Direct Gene Expression?," *Progress in Clinical and Biological Research* 249 (1987): 251–262.

16. A. Costa, J. D. Naranjo, R. Londono, and S. F. Badylak, "Biologic Scaffolds," *Cold Spring Harbor Perspectives in Medicine* 7, no. 9 (2017): a025676, https://doi.org/10.1101/cshperspect.a025676.

17. K. P. Robb, A. Shridhar, and L. E. Flynn, "Decellularized Matrices as Cell-Instructive Scaffolds to Guide Tissue-Specific Regeneration," *ACS Biomaterials Science & Engineering* 4, no. 11 (2018): 3627–3643, https://doi.org/10.1021/acsbiomaterials.7b00619.

18. C. Frantz, K. M. Stewart, and V. M. Weaver, "The Extracellular Matrix at a Glance," *Journal of Cell Science* 123, no. Pt 24 (2010): 4195–4200, https://doi.org/10.1242/jcs.023820.

19. A. V. Bryksin, A. C. Brown, M. M. Baksh, M. G. Finn, and T. H. Barker, "Learning From Nature - Novel Synthetic Biology Approaches for Biomaterial Design," *Acta Biomaterialia* 10, no. 4 (2014): 1761–1769, https://doi.org/10.1016/j.actbio.2014.01.019.

20. D. E. Heath, "A Review of Decellularized Extracellular Matrix Biomaterials for Regenerative Engineering Applications," *Regenerative Engineering and Translational Medicine* 5, no. 2 (2019): 155–166, https://doi.org/10.1007/s40883-018-0080-0.

21. A. Porzionato, E. Stocco, S. Barbon, F. Grandi, V. Macchi, and R. de Caro, "Tissue-Engineered Grafts From Human Decellularized Extracellular Matrices: A Systematic Review and Future Perspectives," *International Journal of Molecular Sciences* 19, no. 12 (2018): 4117, https://doi.org/10.3390/ijms19124117.

22. O. A. Mohiuddin, B. Campbell, J. N. Poche, et al., "Decellularized Adipose Tissue: Biochemical Composition, In Vivo Analysis and Potential Clinical Applications," *Advances in Experimental Medicine and Biology* 1212 (2020a): 57–70, https://doi.org/10.1007/5584_2019_371.

23. B. S. Kim, S. Das, J. Jang, and D.-W. Cho, "Decellularized Extracellular Matrix-Based Bioinks for Engineering Tissue- and Organ-Specific Microenvironments," *Chemical Reviews* 120, no. 19 (2020): 10608–10661, https://doi.org/10.1021/acs.chemrev.9b00808.

24. L. T. Saldin, M. C. Cramer, S. S. Velankar, L. J. White, and S. F. Badylak, "Extracellular Matrix Hydrogels From Decellularized Tissues: Structure and Function," *Acta Biomaterialia* 49 (2017): 1–15, https://doi.org/10.1016/j.actbio.2016.11.068.

25. P. M. Crapo, T. W. Gilbert, and S. F. Badylak, "An Overview of Tissue and Whole Organ Decellularization Processes," *Biomaterials* 32, no. 12 (2011): 3233–3243, https://doi.org/10.1016/j.biomaterials.2011.01.057.

26. T. J. Keane, I. T. Swinehart, and S. F. Badylak, "Methods of Tissue Decellularization Used for Preparation of Biologic Scaffolds and In Vivo Relevance," *Methods (San Diego, Calif.)* 84 (2015): 25–34, https://doi.org/10.1016/j.ymeth.2015.03.005.

27. A. Gilpin and Y. Yang, "Decellularization Strategies for Regenerative Medicine: From Processing Techniques to Applications," *BioMed Research International* 2017 (2017): 9831534, https://doi.org/10.1155/2017/9831534.

28. U. Mendibil, R. Ruiz-Hernandez, S. Retegi-Carrion, N. Garcia-Urquia, B. Olalde-Graells, and A. Abarrategi, "Tissue-Specific

Decellularization Methods: Rationale and Strategies to Achieve Regenerative Compounds," *International Journal of Molecular Sciences* 21, no. 15 (2020): 5447, https://doi.org/10.3390/ijms21155447.

29. L. E. Flynn, "The Use of Decellularized Adipose Tissue to Provide an Inductive Microenvironment for the Adipogenic Differentiation of Human Adipose-Derived Stem Cells," *Biomaterials* 31, no. 17 (2010): 4715–4724, https://doi.org/10.1016/j.biomaterials.2010.02.046.

30. J.-Z. Yang, L.-H. Qiu, S.-H. Xiong, et al., "Decellularized Adipose Matrix Provides an Inductive Microenvironment for Stem Cells in Tissue Regeneration," *World Journal of Stem Cells* 12, no. 7 (2020): 585–603, https://doi.org/10.4252/wjsc.v12.i7.585.

31. Y. C. Choi, J. S. Choi, B. S. Kim, J. D. Kim, H. i. Yoon, and Y. W. Cho, "Decellularized Extracellular Matrix Derived From Porcine Adipose Tissue as a Xenogeneic Biomaterial for Tissue Engineering," *Tissue Engineering. Part C, Methods* 18, no. 11 (2012): 866–876, https://doi.org/10.1089/ten.TEC.2012.0009.

32. B. S. Kim, J. S. Choi, J. D. Kim, Y. C. Choi, and Y. W. Cho, "Recellularization of Decellularized Human Adipose-Tissue-Derived Extracellular Matrix Sheets With Other Human Cell Types," *Cell and Tissue Research* 348, no. 3 (2012): 559–567, https://doi.org/10.1007/s00441-012-1391-y.

33. L. Wang, J. A. Johnson, Q. Zhang, and E. K. Beahm, "Combining Decellularized Human Adipose Tissue Extracellular Matrix and Adipose-Derived Stem Cells for Adipose Tissue Engineering," *Acta Biomaterialia* 9, no. 11 (2013a): 8921–8931, https://doi.org/10.1016/j.actbio.2013.06.035.

34. L. E. Kokai, B. K. Schilling, E. Chnari, et al., "Injectable Allograft Adipose Matrix Supports Adipogenic Tissue Remodeling in the Nude Mouse and Human," *Plastic and Reconstructive Surgery* 143, no. 2 (2019): 299e–309e, https://doi.org/10.1097/PRS.0000000000005269.

35. F. Pati, D.-H. Ha, J. Jang, H. H. Han, J.-W. Rhie, and D.-W. Cho, "Biomimetic 3D Tissue Printing for Soft Tissue Regeneration," *Biomaterials* 62 (2015): 164–175, https://doi.org/10.1016/j.biomaterials.2015.05.043.

36. Q.-W. Tan, Y. Zhang, J.-C. Luo, et al., "Hydrogel Derived From Decellularized Porcine Adipose Tissue as a Promising Biomaterial for Soft Tissue Augmentation," *Journal of Biomedical Materials Research. Part A* 105, no. 6 (2017): 1756–1764, https://doi.org/10.1002/jbm.a.36025.

37. A. E. B. Turner, C. Yu, J. Bianco, J. F. Watkins, and L. E. Flynn, "The Performance of Decellularized Adipose Tissue Microcarriers as an Inductive Substrate for Human Adipose-Derived Stem Cells," *Biomaterials* 33, no. 18 (2012): 4490–4499, https://doi.org/10.1016/j.biomaterials.2012.03.026.

38. H. K. Cheung, T. T. Y. Han, D. M. Marecak, J. F. Watkins, B. G. Amsden, and L. E. Flynn, "Composite Hydrogel Scaffolds Incorporating Decellularized Adipose Tissue for Soft Tissue Engineering With Adipose-Derived Stem Cells," *Biomaterials* 35, no. 6 (2014): 1914–1923, https://doi.org/10.1016/j.biomaterials.2013.11.067.

39. C. Yu, J. Bianco, C. Brown, et al., "Porous Decellularized Adipose Tissue Foams for Soft Tissue Regeneration," *Biomaterials* 34, no. 13 (2013): 3290–3302, https://doi.org/10.1016/j.biomaterials.2013.01.056.

40. D. Adam Young, V. Bajaj, and K. L. Christman, "Award Winner for Outstanding Research in the PhD Category, 2014 Society for Biomaterials Annual Meeting and Exposition, Denver, Colorado, April 16–19, 2014: Decellularized Adipose Matrix Hydrogels Stimulate In Vivo Neovascularization and Adipose Formation," *Journal of Biomedical Materials Research. Part A* 102, no. 6 (2014): 1641–1651, https://doi.org/10.1002/jbm.a.35109.

41. Q.-W. Tan, S.-L. Tang, Y. Zhang, et al., "Hydrogel From Acellular Porcine Adipose Tissue Accelerates Wound Healing by Inducing Intradermal Adipocyte Regeneration," *Journal of Investigative Dermatology* 139, no. 2 (2019): 455–463, https://doi.org/10.1016/j.jid.2018.08.013.

42. B. N. Brown, J. M. Freund, L. Han, et al., "Comparison of Three Methods for the Derivation of a Biologic Scaffold Composed of Adipose Tissue Extracellular Matrix," *Tissue Engineering. Part C, Methods* 17, no. 4 (2011): 411–421, https://doi.org/10.1089/ten.TEC.2010.0342.

43. H. Sano, H. Orbay, H. Terashi, H. Hyakusoku, and R. Ogawa, "Acellular Adipose Matrix as a Natural Scaffold for Tissue Engineering," *Journal of Plastic, Reconstructive & Aesthetic Surgery: JPRAS* 67, no. 1 (2014): 99–106, https://doi.org/10.1016/j.bjps.2013.08.006.

44. C. Thomas-Porch, J. Li, F. Zanata, et al., "Comparative Proteomic Analyses of Human Adipose Extracellular Matrices Decellularized Using Alternative Procedures," *Journal of Biomedical Materials Research. Part A* 106, no. 9 (2018): 2481–2493, https://doi.org/10.1002/jbm.a.36444.

45. O. A. Mohiuddin, J. M. Motherwell, E. Rogers, et al., "Characterization and Proteomic Analysis of Decellularized Adipose Tissue Hydrogels Derived From Lean and Overweight/Obese Human Donors," *Advanced Biosystems* 4, no. 10 (2020b): e2000124, https://doi.org/10.1002/adbi.202000124.

46. S. F. Badylak, "Decellularized Allogeneic and Xenogeneic Tissue as a Bioscaffold for Regenerative Medicine: Factors That Influence the Host Response," *Annals of Biomedical Engineering* 42, no. 7 (2014): 1517–1527, https://doi.org/10.1007/s10439-013-0963-7.

47. M. S. Massaro, R. Pálek, J. Rosendorf, L. Červenková, V. Liška, and V. Moulisová, "Decellularized Xenogeneic Scaffolds in Transplantation and Tissue Engineering: Immunogenicity Versus Positive Cell Stimulation," *Materials Science & Engineering. C, Materials for Biological Applications* 127 (2021): 112203, https://doi.org/10.1016/j.msec.2021.112203.

48. F. Naso, A. Gandaglia, L. Iop, M. Spina, and G. Gerosa, "First Quantitative Assay of Alpha-Gal in Soft Tissues: Presence and Distribution of the Epitope Before and After Cell Removal From Xenogeneic Heart Valves," *Acta Biomaterialia* 7, no. 4 (2011): 1728–1734, https://doi.org/10.1016/j.actbio.2010.11.030.

49. M. Parmaksiz, A. Dogan, S. Odabas, A. E. Elçin, and Y. M. Elçin, "Clinical Applications of Decellularized Extracellular Matrices for Tissue Engineering and Regenerative Medicine," *Biomedical Materials (Bristol, England)* 11, no. 2 (2016): 22003, https://doi.org/10.1088/1748-6041/11/2/022003.

50. D. S. Masson-Meyers and L. Tayebi, "Vascularization Strategies in Tissue Engineering Approaches for Soft Tissue Repair," *Journal of Tissue Engineering and Regenerative Medicine* 15, no. 9 (2021): 747–762, https://doi.org/10.1002/term.3225.

51. P. Bainbridge, "Wound Healing and the Role of Fibroblasts," *Journal of Wound Care* 22, no. 8 (2013): 407–412, https://doi.org/10.12968/jowc.2013.22.8.407.

52. R. Edri, I. Gal, N. Noor, et al., "Personalized Hydrogels for Engineering Diverse Fully Autologous Tissue Implants," *Advanced Materials (Deerfield Beach, Fla.)* 31, no. 1 (2019): e1803895, https://doi.org/10.1002/adma.201803895.

53. W. Wang, B. Cao, L. Cui, J. Cai, and J. Yin, "Adipose Tissue Engineering With Human Adipose Tissue-Derived Adult Stem Cells and a Novel Porous Scaffold," *Journal of Biomedical Materials Research. Part B, Applied Biomaterials* 101, no. 1 (2013b): 68–75, https://doi.org/10.1002/jbm.b.32816.

54. P. Morissette Martin, A. Shridhar, C. Yu, C. Brown, and L. E. Flynn, "Decellularized Adipose Tissue Scaffolds for Soft Tissue Regeneration and Adipose-Derived Stem/Stromal Cell Delivery," *Methods in Molecular Biology (Clifton, N.J.)* 1773 (2018): 53–71, https://doi.org/10.1007/978-1-4939-7799-4_6.

55. D. D. Cissell, J. M. Link, J. C. Hu, and K. A. Athanasiou, "A Modified Hydroxyproline Assay Based on Hydrochloric Acid in Ehrlich's Solution Accurately Measures Tissue Collagen Content," *Tissue Engineering. Part C, Methods* 23, no. 4 (2017): 243–250, https://doi.org/10.1089/ten.tec.2017.0018.

56. S. F. Badylak, D. O. Freytes, and T. W. Gilbert, "Extracellular Matrix as a Biological Scaffold Material: Structure and Function," *Acta*

Biomaterialia 5, no. 1 (2009): 1–13, https://doi.org/10.1016/j.actbio.2008.09.013.

57. M. Heller, H.-K. Bauer, R. Schwab, et al., "The Impact of Intercellular Communication for the Generation of Complex Multicellular Prevascularized Tissue Equivalents," *Journal of Biomedical Materials Research. Part A* 108, no. 3 (2020): 734–748, https://doi.org/10.1002/jbm.a.36853.

58. H.-K. Bauer, D. Flesch, S. Walenta, et al., "Primary Mucosal Epithelial Cell Cultivation: A Reliable and Accelerated Isolation," *Tissue Engineering. Part C, Methods* 25, no. 2 (2019): 82–92, https://doi.org/10.1089/ten.tec.2018.0327.

59. L. Benning, L. Gutzweiler, K. Tröndle, et al., "Cytocompatibility Testing of Hydrogels Toward Bioprinting of Mesenchymal Stem Cells," *Journal of Biomedical Materials Research. Part A* 105, no. 12 (2017): 3231–3241, https://doi.org/10.1002/jbm.a.36179.

60. L. Benning, L. Gutzweiler, K. Tröndle, et al., "Assessment of Hydrogels for Bioprinting of Endothelial Cells," *Journal of Biomedical Materials Research. Part A* 106, no. 4 (2018): 935–947, https://doi.org/10.1002/jbm.a.36291.

61. F. Kubaski, H. Osago, R. W. Mason, et al., "Glycosaminoglycans Detection Methods: Applications of Mass Spectrometry," *Molecular Genetics and Metabolism* 120, no. 1–2 (2017): 67–77, https://doi.org/10.1016/j.ymgme.2016.09.005.

62. C. S. L. Voytik-Harbin, A. O. Brightman, B. Z. Waisner, J. P. Robinson, and C. H. Lamar, "Small Intestinal Submucosa: A Tissue-Derived Extracellular Matrix That Promotes Tissue-Specific Growth and Differentiation of Cells in Vitro," *Tissue Engineering* 4, no. 2 (1998): 157–174. https://doi.org/10.1089/ten.1998.4.157.

63. D. O. Freytes, J. Martin, S. S. Velankar, A. S. Lee, and S. F. Badylak, "Preparation and Rheological Characterization of a Gel Form of the Porcine Urinary Bladder Matrix," *Biomaterials* 29, no. 11 (2008): 1630–1637, https://doi.org/10.1016/j.biomaterials.2007.12.014.

64. F. Zhao, J. Cheng, J. Zhang, et al., "Comparison of Three Different Acidic Solutions in Tendon Decellularized Extracellular Matrix Bio-Ink Fabrication for 3D Cell Printing," *Acta Biomaterialia* 131 (2021): 262–275, https://doi.org/10.1016/j.actbio.2021.06.026.

65. M. B. Burg, J. D. Ferraris, and N. I. Dmitrieva, "Cellular Response to Hyperosmotic Stresses," *Physiological Reviews* 87, no. 4 (2007): 1441–1474, https://doi.org/10.1152/physrev.00056.2006.

66. F. Blaudez, S. Ivanovski, S. Hamlet, and C. Vaquette, "An Overview of Decellularisation Techniques of Native Tissues and Tissue Engineered Products for Bone, Ligament and Tendon Regeneration," *Methods (San Diego, Calif.)* 171 (2020): 28–40, https://doi.org/10.1016/j.ymeth.2019.08.002.

67. B. Sun, "The Mechanics of Fibrillar Collagen Extracellular Matrix," *Cell Reports Physical Science* 2, no. 8 (2021): 100515, https://doi.org/10.1016/j.xcrp.2021.100515.

68. T. Langrock and R. Hoffmann, "Analysis of Hydroxyproline in Collagen Hydrolysates," *Methods in Molecular Biology (Clifton, N.J.)* 2030 (2019): 47–56, https://doi.org/10.1007/978-1-4939-9639-1_5.

69. C. F. C. Brown, J. Yan, T. T. Y. Han, D. M. Marecak, B. G. Amsden, and L. E. Flynn, "Effect of Decellularized Adipose Tissue Particle Size and Cell Density on Adipose-Derived Stem Cell Proliferation and Adipogenic Differentiation in Composite Methacrylated Chondroitin Sulphate Hydrogels," *Biomedical Materials (Bristol, England)* 10, no. 4 (2015): 45010, https://doi.org/10.1088/1748-6041/10/4/045010.

70. J. Taipale and J. Keski-Oja, "Growth Factors in the Extracellular Matrix," *FASEB Journal* 11 (1997): 51–59, https://doi.org/10.1096/fasebj.11.1.9034166.

71. J. E. Reing, B. N. Brown, K. A. Daly, et al., "The Effects of Processing Methods Upon Mechanical and Biologic Properties of Porcine Dermal Extracellular Matrix Scaffolds," *Biomaterials* 31, no. 33 (2010): 8626–8633, https://doi.org/10.1016/j.biomaterials.2010.07.083.